Feasibility Assessment

of motion compensated cranes

at an early design stage

Mark **Driessen**

TU Delft

Feasibility assessment of motion compensated cranes at an early design stage

by

M.P.J. Driessen

to obtain the degree of Master of Science
at the Delft University of Technology,
to be defended publicly on Thursday September 30, 2021 at 1:00 PM.

Student number:	4443446	
Project duration:	October 1, 2020 – October 1, 2021	
Thesis committee:	Dr. ir. H. HosseinNia,	TU Delft
	Dr. ir. F. Alijani,	TU Delft
	Ir. J. Los,	Huisman Equipment, supervisor

TU Delft

To my mother and Tessa, the two most beautiful persons in the world

Abstract

Current service and installation activities to offshore wind turbines (OWTs) are mainly carried out by jack-up vessels. These vessels vessels are less susceptive to disturbances caused by sea waves when they lift their hull from the water level by jacking down multiple legs to the seabed. An alternative is a crane mounted on a floating vessel, which has the benefits of being faster regarding sailing time, cheaper in operation, able to locate multiple times around the same offshore site and able to operate in deep waters. However floating crane vessels have a significant lower workability in comparison to jack-up vessels and are therefore not deployed in OWT activities yet.

Huisman initiated the three-dimensional (3D) motion compensated crane (MCC) project to improve the workability of crane vessels in offshore operations - thereby focusing on the performance of the equipped cranes - such that floating crane vessels will be able to install and service OWTs during an sufficiently large operational window. But to date MCCs have never been realized for offshore wind industry, which makes it difficult to estimate their performance beforehand and evaluate whether they are feasibile.

This thesis describes the development of a procedure to assess the feasibility of motion systems from a mechatronic design perspective and the motion compensation system of the Huisman 3D MCC is used as a case study. Several aspects of the MCC have been studied into more detail because these aspects are an determining factor regarding feasibility. These aspects are the influence of actuator type and crane boom flexibility and the performance during realistic offshore conditions. To investigate these aspects the system dynamics of the conceptual design are modelled, a controller is designed for the model and parameters are identified. Next the model is evaluated on its disturbance rejection capability because this is an important performance indicator for motion compensation, its robustness is examined and whether the OWT installation requirements are fulfilled.

Acknowledgements

Last year has been exciting and hectic sometimes, but above all very educational. Due to several great persons I have been able to write the work in front of you. Therefore I would like to thank my colleagues at Huisman first, in particular Jan and Ashley.

Furthermore I would like to thank Hassan and the other members of the group for the important moments of reflection. Many interesting projects have been come by last year.

Special thanks to Mo, with whom I had many meetings even during weekends sometimes. Good luck with finishing your thesis.

Tom for the cover design.

The high-tech party! We had many nice moments during our first year and an unforgettable trip last summer.

Finally, I would like to thank my family, friends and Tessa for their support and necessary distraction. I feel very fortunate to have you in my life.

M.P.J. Driessen
Delft, September 2021

Contents

List of abbreviations

DOF	Degree of Freedom
JONSWAP	Joint North Sea Wave Project
MCC	Motion Compensated Crane
MCS	Motion Compensation System
MRU	Motion Reference Unit
OWT	Offshore Wind Turbine
PID	Proportional Integral Derivative
PMOC	Pedestal Mounted Offshore Crane
RAO	Response Amplitude Operator

Nomenclature

m_t	$Trolleymass$	kg
J_m	$Motorinertia$	$kg \cdot m^2$
n_m	$Numberofmotors$	$-$
i_g	$Numberofgearboxes$	$-$
J_g	$Gearboxinertia$	$kg \cdot m^2$
T_2	$Torque$	Nm
ζ	$Dampingratio$	$-$
m	$Gearingteethmodulus$	m
n_g	$Numberofgearingteeth$	$-$
n_p	$Numberofpinionteeth$	$-$
n_{rp}	$Numberofrack-and-piniondrives$	$-$
m_{boom}	$Craneboommass$	kg
L_{boom}	$Craneboomlength$	m
k_{boom}	$Effectivecraneboomstiffness$	$\frac{N}{m}$
c_{boom}	$Effectivecraneboomdamping$	$\frac{N \cdot s}{m}$
β	$Craneboomangle$	deg
N_{falls}	$Numberoffallsinboomhoistrope$	$-$
E_{eff}	$EffectiveYoung'smodulus$	Pa
A_{rope}	$Areaofboomhoistrope$	m^2
$L_{boomhoist}$	$Lengthofboomhoistrope$	m
γ	$Anglebetweenluffingframeandboomhoistrope$	deg
η	$Boomhoistropeangle$	deg
θ	$Craneboomangle$	deg
T_p	$Peakperiod$	s
H_s	$Significantwaveheight$	m
S_ζ	$Waveenergyresponse$	$m^2 \cdot s$
$m_{n\zeta}$	$n-thorderspectralmoment$	m^2
$H_{1/3}$	$Significantresponseheight$	m
f	$Frequency$	Hz

List of Figures

List of Tables

1 Introduction

The development of motion systems for offshore cranes shows an increasing level of complexity that requires engineers to use feasibility checks to assess the preliminary performance of concepts at an early stage of the design process. The reasoning behind this approach is to prevent the rise of unnecessary development costs although be able to still achieve first-time-right designs and assure quality of the product. This thesis report describes the development of that feasibility test. The machine in question does not have any readily 'off-the-shelf' feasibility checks available and there is little knowledge and experience in developing these tests. This invites to perform academic research to the possibilities for such feasibility tests. This chapter will provide an introduction to the study by first discussing the background and problem statement, followed by the research scope and purpose.

1.1. Background

To secure the energy demand the industry desires to build, install and operate offshore wind turbines (OWTs). Simultaneous to the increase of installed offshore wind capacity, the demand for service and repair grows as well because OWTs occasionally fail during their desired operating period. Both installation and service activities require a difficult lifting operation that is challenged by several developments:

- Due to the increasing size of OWTs the installation and service activities become more difficult. The increased turbine hub height and increased weight of turbine parts affect the operational window because cranes are pushed towards their lift capacity limits and can thus only operate in mild environmental conditions. This is proven by Verma et al, who show based on statistical data from others that 53% of the installation time is spent on waiting for suitable environmental conditions [1] [2]. Using larger crane vessels that can operate under more severe environmental conditions is possible, but comes with the disadvantage of additional costs.

- The wind turbine market desires to be able to operate all year around. This is largely dependent on local sea states, for instance the North Sea does not allow to install or replace OWTs during most time of the year. This means that the growth of the offshore wind market could be limited. Another consideration is that rough sea states limit the possibility to service and repair OWTs, which results in an increased down-time of OWTs [3].

Current service and installation activities to offshore wind turbines are mainly carried out by jack-up vessels as can be seen in figure 1.1 and figure 1.2a. Jack-up vessels are less susceptive to disturbances caused by sea waves when they lift their hull from the water level by jacking down multiple legs to the seabed. An alternative is a crane mounted on a floating vessel, which has several benefits when compared to jack-up vessels:

- Floating, especially mono-hull vessels illustrated in 1.2b, can perform operations quicker since they have a higher sail speed and do not need to jack-up, an activity that takes a couple of hours [5] [6], or submerse themselves, illustrated in 1.2c. This characteristic is important for repair operations when service vessels need to sail for one or few OWTs exclusively.

Figure 1.1: Jack-up vessel aligning the OWT blade for installation in an offshore wind park. Adapted from [4]

- Jack-up vessels cannot position on bad soil conditions of the sea bottom. Furthermore they cannot operate too many times around an offshore structure because the seabed is weakened and leave elephant marks on the sea bottom after the legs are retracted [6] [7].
- Most jack-up vessels cannot operate in deep waters to service floating OWTs because of their sea depth limit related to the length of their legs [6] [7] [3].

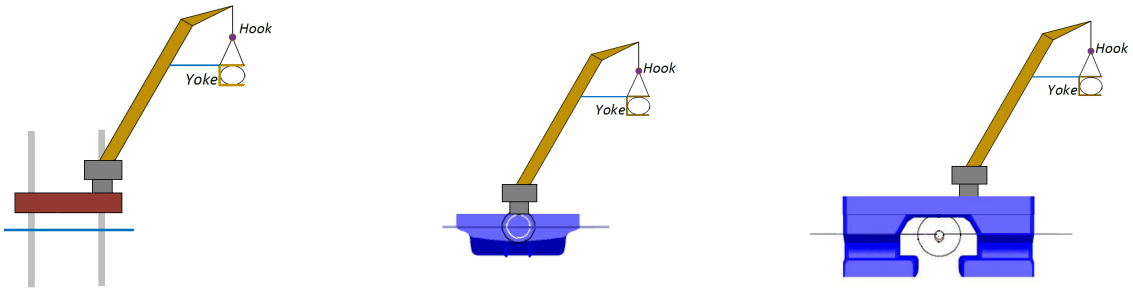

(a) (b) (c)

Figure 1.2: Side view of common crane vessel types and notation of yoke-hook assembly. Adapted from [7] (a): Jack-up vessel (b): Monohull vessel (c): Semi-submersible vessel

Thus it is appealing to use floating crane vessels for the mentioned tasks, however the significant lower workability in comparison to jack-up vessels is a serious drawback. Therefore Huisman initiated the three-dimensional (3D) motion compensated crane (MCC) project. The purpose of this project is to improve the workability of crane vessels in offshore operations - thereby focusing on the performance of the equipped cranes - such that floating crane vessels will be able to install and service OWTs during an sufficiently large operational window.
Huisman developed two MCC concepts, a positioning table and a cable-driven parallel robot concept. A detailed description of these concepts will be given in Section 2.2.4. Both concepts have their motion compensation system (MCS) located at the crane tip. Prior research into compensation systems located at the crane base shows that this principle is infeasible because the compensation system needs to move the high weight of the entire crane structure and its load. Working MCCs exist, but these cranes have a limited load

capacity (< 10 T) and low working height. These cranes differ considerable from the MCC intended for OWT installation and therefore it is still uncertain whether the latter is feasible regarding motion compensation performance.

1.2. Problem statement and motivation

MCCs could offer an outcome to the issue of low workability performance of floating crane vessels, but to date MCCs have never been realized for offshore wind industry which makes it difficult to estimate their performance beforehand and evaluate whether it is an improvement [8]. Thus because of limited experience and knowledge with such cranes and due to the complex mechatronic system behind the motion compensated crane it is preferable to perform a feasibility check of its conceptual designs at an early stage of the design process. Several arguments motivate this feasibility check:

- It is a quality predictor that can estimate performance. Thus it will prevent putting too much effort in detailed modeling of perhaps infeasible concepts.
- It is possible to make design changes at relatively low costs given the fact that the check has been performed at an early design stage.
- It becomes possible to assess multiple concepts and choose the best one for the same costs as the old method where only one concept was developed and assessed. This is because the feasibility check is performed at an early design stage when the development costs are not high yet.
- It improves the overall design process because it tries to obtain fundamental insight of the concept. This will facilitate making design decisions, which can eventually reduce development time and costs.

Assessing feasibility is thus reasonable from both economic and technical perspectives. In the engineering discipline, feasibility is related to technical aspects of concepts, designs or complete systems and can be considered as the measure of fulfilment of requirements. Thus the methods to assess this must be able to analyse, compare or quantify the characteristics of the concept. There are several challenges involved with feasibility assessment that could influence the accuracy and reliability of the results:

- Mechatronic design entails multiple physical domains, such as mechanical, electrical and hydraulics, thus requirements arise from diverse perspectives and in order to assess the feasibility correctly, the requirements need to be compatible. This could mean that requirements need to be transformed to other physical domains to encorporate them in the design process. In practice, this means that:
  - Analysis of physical mechanisms and phenomena or the behavior that it causes is required to understand how requirements and design specifications can be fulfilled.
  - Clear and compatible feasibility criteria, baseline and assessment methods are required that can be used at top level engineering to prevent having to go to much in detail.
- Feasibility test must be performed at early design stage, which means that the design is barely specified. Hopefully requirements are defined since this gives conditions for the feasibility assessment method.
- Fully specified designs can be implemented into simulation software and provide answers regarding performance, durability or feasibility. However this is more complicated for conceptual designs because the designs are not fully specified yet, which means that they can only be assessed to a limited extent. Therefore only fundamental principles can be applied in order to assess the feasibility. Note that these using these methods will probably result in a lower degree of accuracy and reliability.

In addition there are challenges more specifically related to the MCC. From several equipment characteristics it is expected that they will have a major influence on the performance and thus the feasibility of the system. Therefore it is essential to take into account these characteristics during the feasibility assessment. From preliminary research and discussion within Huisman it appears that the flexibility of the crane boom is very relevant, since boom motions will cause additional disturbances that have to be compensated. In addition the actuator type has influence on the performance due to the specific actuator dynamics. Besides equipment characteristics the behavior of disturbances, how this acts on the vessel and the vessel-crane interaction are important to consider. This relates to how well disturbances are rejected by the motion compensation system and is a good indicator of the motion compensation performance.

1.3. Research scope and purpose

It has become evident that the feasibility test is an useful tool during the design process of mechatronic systems. However no tests are available yet and this motivates to perform academic research with the purpose to assess the feasibility of the proposed 3D MCC concepts at an early design stage. During system evaluation characteristics have been identified that demand revision and further specification of the research objective. In the context of feasibility assessment the following objectives are relevant for this study:

- Compare the performance of MCC with different actuator types to investigate the influence of actuator flexibility and dynamics.
- Investigate the influence of crane boom flexibility.
- Quantify the performance of the MCC for realistic offshore conditions to check whether the operational requirements of OWT activities are fulfilled.

The scope of this study is limited to:

- Installation of offshore wind turbine blades is chosen as the operational scope.
- The considered vessel type is a mono-hull.
- The crane of interest is pedestal mounted. It is characterized by its long vertical boom.
- Only the positioning table concept at the crane tip is assessed in this study, but a brief introduction to the other concept will be given.

The focus defines the direction of research and is given by the following statements:

- The assessment procedure is not used to optimize the design, it is focused on assessment.
- The first priority of the research is to establish an analytical method that is based on fundamental principles in mechatronic system design. By doing this, understanding of the principles is developed.
- After this method has been established, the focus of the practical research shifts towards investigation of identified dynamic effects that could degrade the performance of the MCC and affect the feasibility. Literature study and discussion within Huisman shows that these effects are relevant and require further research.

1.4. Report structure

Chapter Two treats the evaluation of the system. The OWT blade installation activity will be examined, the MCC concepts will be described and the performance test is regarded. Chapter Three explains the modelling steps, assumptions and conditions based on the research objectives. Chapter Four shows the results. Chapter Five contains the conclusions. Chapter Six discusses the research process and findings and gives recommendations for further research.

2

System evaluation

The goal is to assess the performance of the proposed MCC concepts while at this moment it is not clear what these concepts entail and what is meant with performance. Therefore first the task of the MCC will be considered, namely OWT installation and service. To better understand this task, the requirements, operational conditions and installation method are investigated. Then the proposed concepts are examined with respect to their characteristics and differences between the concepts. Finally, the performance test will be regarded. An approach is proposed and important characteristics are taken into account.

2.1. OWT installation requirements

Installation and maintenance activities of OWTs is becoming more important because there is an increasing amount of OWTs and the reliance on OWTs by the energy sector increases as well. The installation procedure and forthcoming operational requirements will be described.

2.1.1. Installation procedure

The most common method nowadays is to transport blade and turbine parts on board the crane vessel. In almost any lifting operation, jack-up vessels are used and floating vessels are rarely seen due to their significant lower workability. After the jack-up vessel is positioned on the site, the legs are jacked-up and blade installation starts according to the following procedure:

1. Fasten yoke to the blade. The yoke is a tool suspended onto the crane to grab the blades without damage and illustrated in figure 2.1a. The yoke can rotate by using tugger lines, which are attached to the crane boom.

2. Lift blade to hub height. Control orientation with tugger lines.

3. Align blade root with hub. This is illustrated in figure 2.1b. Carefully move blade towards hub by crane and tugger operation. Monitor blade root motion to decide whether mating is possible according to safety margins. Suspend blade with hub to prevent swinging.

4. Mate blade root with hub. This activity takes a couple of hours, thus there is risk for weather changes. Blade should not swing too much otherwise blade root already gets damaged or bolts are not tensioned well.

5. Detach yoke and return to deck for installation of next blade, other turbine parts or move to next offshore site or port.

Step 3 is critical because the blade and guiding pins can get damaged and if this happens no installation is possible and blade or pins need to be replaced. Step 4 also carries considerable amount of risk when weather changes and blade is not fully mated yet.
Motion compensation offers a solution to fulfill the installation tasks under more severe environmental conditions or with more positioning accuracy to reduce the risk for damage. Previous studies and user experience show that blade motion is a serious problem [9] [7] [6].

(a) (b)

Figure 2.1: Blade installation procedure (a): Yoke system for hydraulic clamping of the blade. Adapted from [10] (b): Close-up of the alignment phase. Adapted from [11]

2.1.2. Operational requirements

The alignment and mating phase sets high requirements to the positioning accuracy of the MCS because the blade, its bolts or the turbine can get damaged when parts hit each other with high impact. Currently the alignment is manually coordinated; human operators pull the blade towards the hub with ropes and this creates safety risks. Motion compensation can make the manual coordination of blades unnecessary, which in addition will decrease the safety risks. Positional accuracy is certainly one of the most important characteristics of the installation procedure. This is a serious challenge since the guide pin measures about 4 centimeters in diameter. The tolerance of the hole is smaller than 1 centimeter while the blade measures over 50 meter in length and is installed at a height of 125 meter above sea level [7] [12] [13]. New generation OWTs even have hub heights up to 150 meter [14]. These numbers show the challenge of the installation procedure. Not only the installation of blades requires high positional accuracy; also the replacement of parts inside the turbine nacelle needs this.
Literature does not give clear installation requirements, but from discussions within Huisman and with common sense it is logic that the blade motion should not exceed 10 centimeters of amplitude.
In this study it is assumed that the blade is always right underneath the MCS at the crane tip. For this reason the tugger lines are idealised because in reality the blade is able to swing due to disturbances and the difficulty to keep blade swing down with the tugger winches. Tugger lines run from the crane boom to the yoke-hook assembly and are used to orientate the payload and reduce swing. This simplification has been done because modelling of the moving blade and active tugger control would cost too much time, given the complex geometry of multiple hoisting ropes. To still be able to assess the performance of the MCC the requirement for blade motion will also be used for the MCS.

2.2. Motion compensated crane concepts

An important step within system evaluation is breaking down and understanding the proposed concepts for the MCCs. In this section the characteristics of the concepts and differences between concepts will be described. Furthermore the shortcomings and weaknesses of the concepts are discussed and whether this challenges its feasibility. These findings motivate further research.

2.2.1. Vessel type

Huisman proposed to use the Bokalift 1 as the preliminary crane vessel design because this vessel will be similar to future offshore wind mono-hull vessels. It is illustrated in figure 2.2. The Bokalift 1 is a transportation and installation vessel owned by Boskalis and equipped with a 3000 mT Huisman offshore mast crane. The characteristics that describe the transfer of disturbance mechanisms, such as sea waves, through the vessel towards the crane and suspended load is relevant for the feasibility study.

Figure 2.2: The Bokalift 1 crane vessel is used as the hull shape for vessel motion analysis in this study. Note that the crane in this illustration is not similar to the MCC because it cannot be used in OWT blade installation activities

2.2.2. Crane design

The motion compensation system is mounted to a pedestal mounted offshore crane (PMOC), which is slightly re-designed with a wide boom to decrease its sensitivity to resonances. Figure 2.3a shows a typical PMOC. The motion compensation system possess an own hoist block. In this manner the main hoist can be used for conventional load handling tasks that require more capacity. This crane type is used for many different offshore operations and is the current standard within offshore wind industry because the design is extremely suitable to achieve large lifting heights while it maintains a relatively low construction weight.

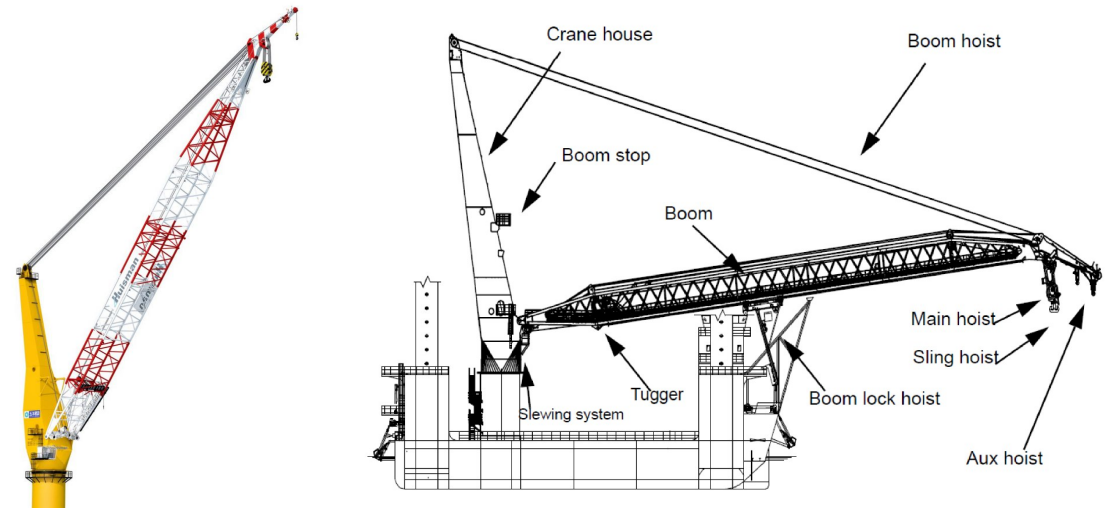

Figure 2.3: Illustrations of PMOCs. (a): Huisman built PMOC (b): Schematic of a PMOC on a jack-up with terminology

2.2.3. Crane boom

The boom consists of two lattice truss structures that join together underneath at the boom pivot and on top at the boom head, as can be seen in figure 2.3. The boom is raised in the correct position by the boom hoist,

which runs to the top of the crane house. This is illustrated in figure 2.3. The boom hoist contains multiple reevings because it carries a substantial load. The tugger system is mounted to the boom. The goal of these tugger winches is to stabilise the load during hoisting and lowering. The system can move towards the correct working height on rails attached to the boom such that the tugger rope can remain horizontal and thus will be loaded under a favorable angle. During transport the boom rests at the boom lock.
The boom head consists of the hoist blocks of which one main block and one or two auxiliary hoists. The main hoist is attached closest to the crane-tip because it must have the highest load capacity. Possibly the auxiliary hoist can be mounted at a fly-jib to reach even higher working heights. The boom head also consists of the motion compensation system that will be described next.
The crane house contains the attachment point of the boom hoist rope and this is why it is such a tall construction. An alternative is the A-frame, which is bolted on a pedestal via the slew bearing and characterized by its open construction. All the important equipment such as winches, electrical cabinets and hydraulic units are located in the closed housing to protect it from the harsh marine environment. This improves the reliability of the equipment and decreases maintenance. It also bears the passive or active heave compensation systems, which can be used to compensate the vertical displacement of the load. An operator cabin is mounted at a side of the crane.
The boom pivot and pedestal with the crane house are mounted on the crane's slew bearing. It is built from multiple segments allowing easy inspection and maintenance. By using a slew bearing the crane does not require a kingpin for transferring the horizontal loads. In addition the slew bearing must withstand the overturning moment of the crane and simultaneously be able to rotate. The slewing system is driven by either hydraulics or electrical.

2.2.4. Motion compensation system

The motion compensation system is designed to keep the hook at a steady position while the crane and vessel are moving due to wave motions. The system is located at the crane tip, as can be seen in figure 2.4a. During motion compensation, the load can be positioned as normal using the slew and boom controls. Slew and boom movements themselves are not compensated. But it is also possible to move the load a little within the 3D movement compensation frame, however only as much as there is stroke left before running into the end of the MCS frames movement capabilities. This is for example done when the blade is aligned and pushed against the hub to create compliance between the blade and hub and prevent swinging.

2.2.5. Positioning table concept

The positioning table concept consists of a two-axis linear motion stage. Underneath the X-frame (the red/white part visible in figure 2.4b, the Y-frame (black/yellow part) moves that holds the trolley containing the hoisting cables and hoist block. The motion compensation frame is kept parallel to the deck by an automatically controlled tackle, which is also visible in figure 2.4b at the back of the boom and on top of the frame. The operator can control the auxiliary hoist joystick to control the vertical distance for approach and landing, the slew and boom controls for positioning in the horizontal plane. Once landed the control system could switch to a constant tension mode on the auxiliary hoist, keeping the XY trolley on active control.
In the trolley design, the hoist wire is reeved back over the two movement axes of the trolley. Due to this design, the hook height will not change when the X or Y movement is compensated. In fact, the Z compensation and XY compensation can be used completely separate from each other. If the XY compensation fails the Z compensation can continue and vice versa.
The positioning table concept has the following advantages:

- A sufficiently large work range is achievable [15].
- There is experience with positioning table motion systems that share the same working principle, within Huisman as well as within industry, but there is no experience for this particular offshore crane application. This motivates to do research into the working principles behind the system, which could facilitate the design process.

The positioning table concept has the following disadvantages:

- A significant amount of weight is added at the crane tip. Besides decreasing the load capacity of the crane it may also affect the structural performance of the crane, especially when the system is in op-

eration and large masses need to be moved. Research is necessary to obtain understanding of this phenomena.

- The serviceability of this concept is an issue. The location of the system components at the crane tip complicates repairs in case of failure. Therefore this concept needs either outstanding lifetime and reliability performance or redundancy must be ensured.

- The use of tuggers during motion compensation. Multiple winches need to be controlled simultaneously which significantly increases the complexity of the system. This situation is simplified in this study by assuming that the load will not swing and thus tuggers are unnecessary and will not be used.

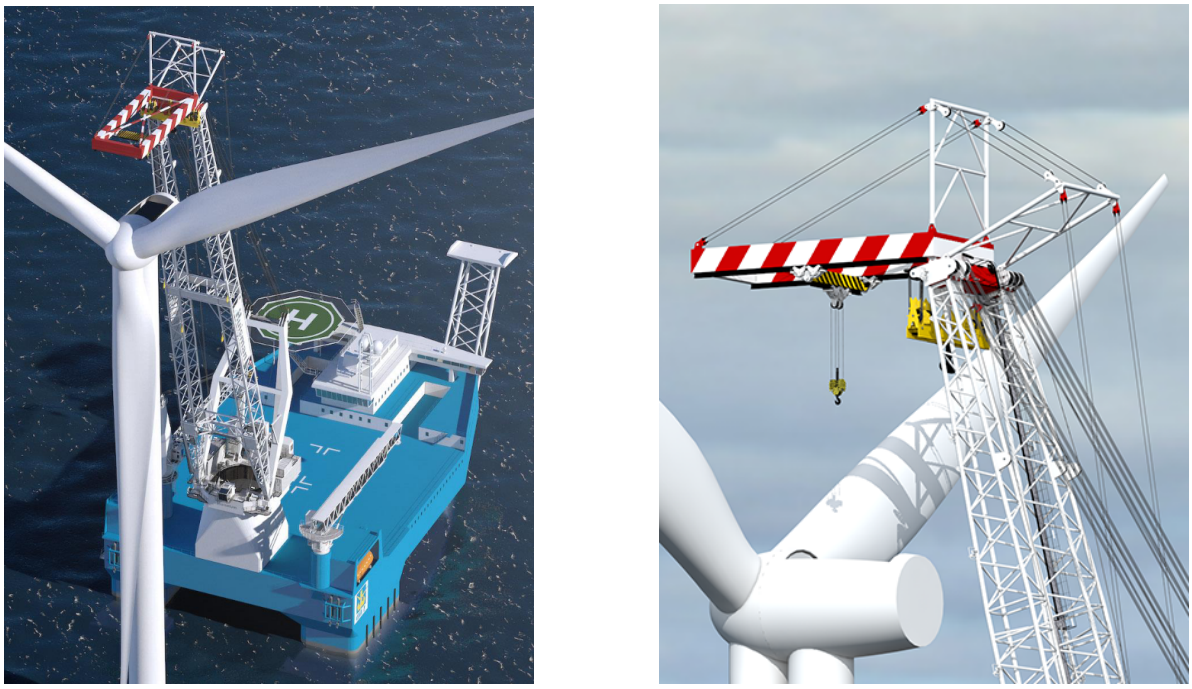

(a) (b)

Figure 2.4: Illustrations of the positioning table system. This illustration shows the replacement of turbine parts in the nacelle, another intended application of the MCC. (a): Overview of crane vessel with positioning table system (b): Close-up of positioning table system

2.2.6. Triple rope concept

The triple rope concept illustrated in figure 2.5 realises 3D compensation by utilizing three cable-drive systems in parallel manipulator configuration. This principle is similar to the cable-driven parallel robots such as used to move suspended cameras in stadiums. The ends of each rope are attached to the end-effector of the system; the hook. The ropes are attached over sheeves that are attached to jibs on top of the crane tip. The orientation of the jibs, and thus the position of the sheeves, makes it possible to move the hook assembly inside a bounded workspace when the ropes are controlled simultaneously.
The triple rope concept has the following advantages:

- Its light weight

- Most moving components can be located at the crane base. This decreases weight at the crane tip and improves serviceability.

The triple rope concept has the following disadvantages:

- Cable wear. During continuous motion compensation operation the wear can become serious and lead to failure. Research is necessary to investigate the severity of cable wear.

- Cable-driven systems have a general issue with loss of tension in cables. This happens when the end-effector makes contact with surrounding structures. This happens for instance when the turbine blade is attached to the hub, but not fully mounted yet. In this situation, the system may not be able to fully compensate for undesired motions because the loss of tension in one or multiple ropes makes the system partly uncontrollable.
- The requirement to control the cable-drive systems simultaneously makes this concept more complex than the positioning table concept regarding control system and controller strategy. It also sets the necessity to have an accurate position signal of the hook assembly.

The triple rope concept will not be assessed in this study because the two concepts are too different to use the same assessment method and the project length does not allow to adjust the method. Furthermore the triple rope concept adds substantially more complexity due to the required control strategy which can be addressed better after acquiring a reliable performance estimation of the positioning table concept.

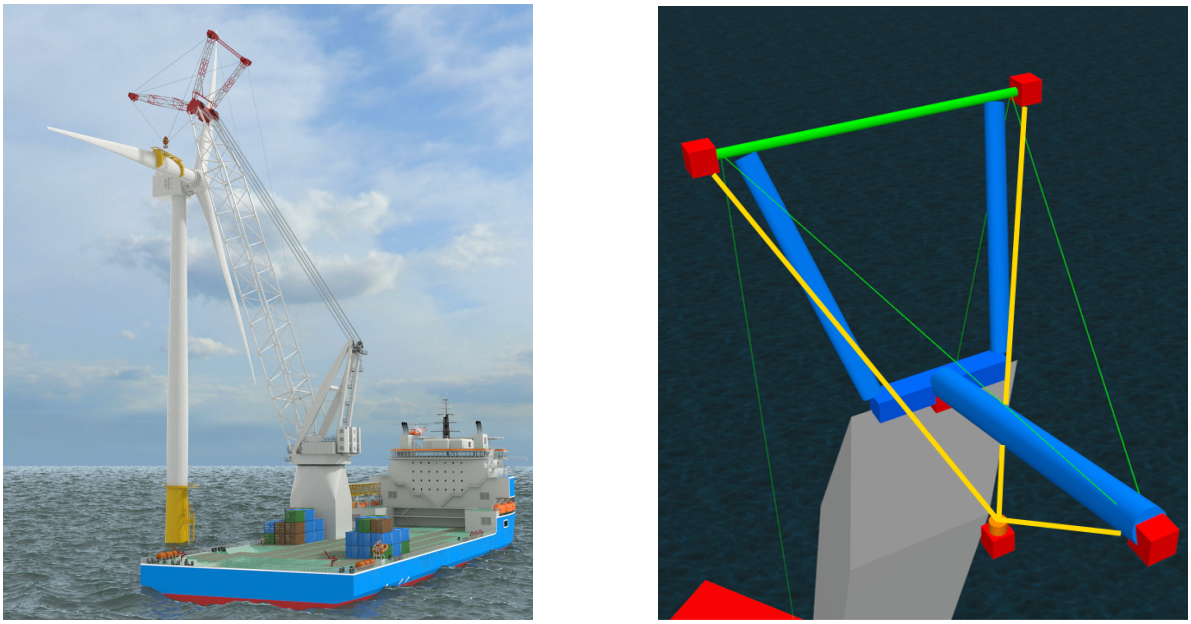

(a) (b)

Figure 2.5: Illustrations of the positioning table system. This illustration shows the replacement of turbine parts in the nacelle, another intended application of the MCC. (a): Overview of crane vessel with triple rope system (b): Close-up of the system showing the three jibs (blue bars), rope sheaves (red box at jib ends), hoist ropes (yellow) and hook-load assembly (red box with orange dot on top)

2.2.7. Actuator types

There are two actuator types available for the positioning table system. This study will show the influence of the actuator type on the system dynamics and check whether it is suitable for use in the MCC.

- A rack and pinion is a linear actuator that consists of a circular gear (the pinion) that engages a linear gear (the rack) to transform rotational motion of the pinion into linear motion. In the MCS the racks are mounted on the X and Y frame. The racks have the property that they can become infinitely long by adding them together. Furthermore the accuracy does not decrease when assembled correctly. The moving parts are the Y frame and the trolley and they carry the motor and gearbox. Several pinions can run over the same toothed rack to execute the movement simultaneously with more force. An essential advantage of rack-pinion systems is that they have almost no backlash. This actuation principle is illustrated in figure 2.6.

- The cable driven system, illustrated in figure 2.7, uses two winches per linear axis to be able to move in both directions. The motor and drum are mounted in the crane house to be able to repair them easily

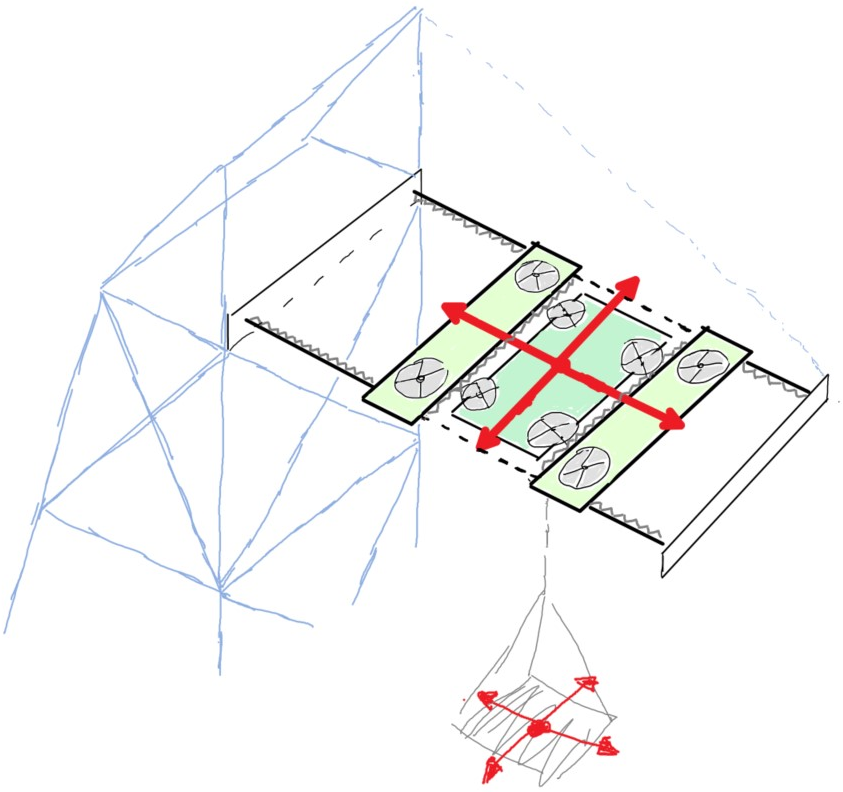

Figure 2.6: Drawing of the positioning table system with rack-and-pinion actuation principle. Light green denotes the X trolley and green the Y trolley. Grey circles represent the pinion gears. Two rack frames are used per direction. Payload hangs underneath the Y trolley and its motion directions (red arrows) correspond to the trolley motion directions

and on top of that it saves weight at the crane tip. Hence a long rope from the crane tip to the crane house is required that could give problems due to the cable stiffness and damping. Besides that cable wear is an issue due to continuous winching during motion compensation mode.

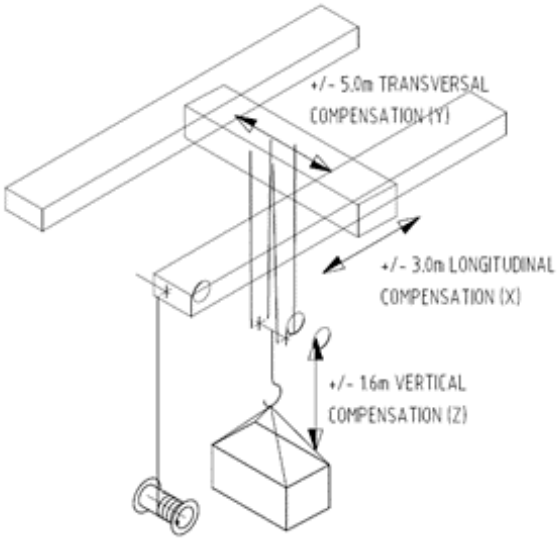

Figure 2.7: Drawing of the positioning table system with cable actuation principle. Note that only one winch is illustrated in this figure, but in reality two winches are required per translational direction

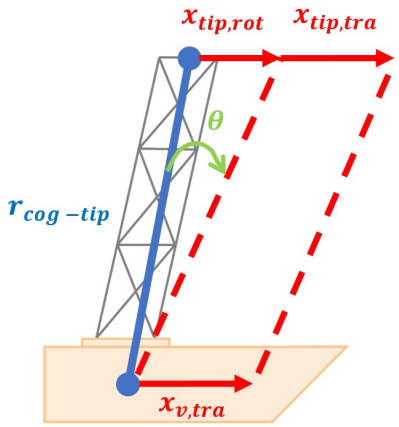

Figure 2.8: Illustration of the crane vessel showing the crane tip disturbances caused by displacement and rotation of the vessel

2.2.8. Motion reference unit

The motion reference unit (MRU) is used for sensing all vessel motions; it measures both angular and linear displacements, velocities and accelerations. Traditionally the MRU is being used in heave compensation solutions thus there is experience with its use and placement, which is typically the vessel COG. The measurements are used to calculate the expected crane tip motion. These calculations would be accurate if the crane were to be completely rigid. However in reality there is crane boom flexibility involved, thus additional crane tip motion is not measured in this manner and differences between the actual tip position and the calculated tip position will occur. For correct motion compensation the exact position needs to be known thus this situation leads to degraded motion compensation performance. The deflection of the boom can be up to 1.5m in the Y direction [4].
The following steps are used to calculate the desired position of the motion compensation trolley with the MRU data:

1. Determine the boom configuration and use this to calculate the transformation vector $r_{cog-tip}$ from vessel COG to crane tip. This will be used to calculate the crane tip displacement due to rotation of the vessel.
2. Calculate the displacement vector of the crane tip due to translational movement of the vessel: $x_{tip,tra} = x_{v,tra}$
3. Calculate the displacement vector of the crane tip due to angular movement of the vessel: $x_{tip,rot} = sin(\theta) \cdot r_{cog,tip}$
4. Sum the displacements: $x_{tip} = x_{tip,rot} + x_{tip,tra}$

2.2.9. Control strategy

The trolley is controlled by two actions: feed forward and feedback. The sea-induced crane tip motions are primarily compensated for by feed forward because this is faster than pure feedback control. The crane tip motions are the disturbances which can be measured by the strategy described in Subsection 2.2.8. The trolley is actuated by speed controlled pinions or winches. The drives of these actuators typically use speed references because the motor speed is measured and fed back to the drive. The feed forward mechanism calculates the desired trolley speed and controls the XY-table DOF and hoist with these reference signals. In this manner most of the desired behavior is achieved by applying feed forward.
Feedback is used to compensate for deficiencies in feed forward, unmeasured disturbances and model uncertainties. Feedback controllers could stabilise and improve the robustness of the controlled system. It will make the system track the desired trajectory by minimising the error between the desired and actual trajectory. This is applied at the desired trolley position in the MCC. The advantage of this approach is prevention of trolley drift such that it hits the end of stroke of the XY-table.
In this study only feedback control is used because this suffices to investigate the influence of dynamics in

actuator and base-frame flexibilities. No complex control strategy is needed to do that. It is difficult to model the feed forward block because it requires knowledge of the drive, amplifier and actuator. Modelling of the feedback control system is treated in Section 3.2.

2.3. Performance test

The disturbance rejection capability is one of the main performance criteria of a motion compensation system. Now that the MCC concept, the conditions and requirements are known, it is possible to assess the system to investigate whether it fulfills the performance criteria. In addition it is interesting to investigate how much the active motion system performs better with respect to the crane without MCS.

2.3.1. Motion system characteristics

Figure 2.9 shows the block diagram of a typical motion system. The goal of this system is to move a part to a desired position. The plant is the uncontrolled physical system and in motion systems it consists of the power amplifier, actuator and mechanical structure, which is the mechanism that transforms input forces and motion into a set of output forces and motion [16]. These three parts each have their own dynamics, which interacts with each other and thus influences the system behavior.

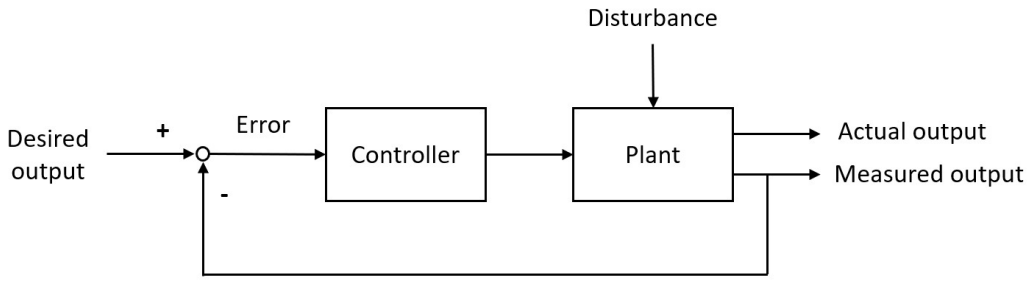

Figure 2.9: System block diagram of a typical motion system

As an illustration consider the very basic motion system in figure 2.10 consisting of a rigid mass, comparable with a moving trolley, that is driven by the actuator force F to move the trolley in similar fashion as a positioning device. Here, the position of the mass x is measured relative to the fixed world, but measuring relative to another reference point is also possible.

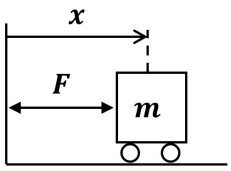

Figure 2.10: Representation of typical motion system consisting of a trolley with mass m that is moved by an actuator with force F. The position x of the trolley is measured and used for control purposes

The plant could experience disturbances from the surrounding environment that will change the output. The output of the system is measured by sensors. Important to know is that in most system the actual output of the system cannot be measured directly because the sensor, such as a rotary encoder at the drive shaft, measures another output. The difference in outputs arises because of elasticity in the mechanical system and imperfections in the transmission of the powertrain and inaccuracy of the encoder [17]. Furthermore the sensor has its own dynamics, which gives uncertainties as well. These sensor dynamics could be taken into account and represented by a block, however these dynamics will not be considered in this study and it can be assumed that the output of the desired end-effector is measured without error. The sensor converts the

analog signal to a digital signal.
The output signal is compared with the desired output. This reference signal could be a motion profile for example. In this system, negative feedback is used and therefore the output tends to reduce fluctuations in the output, which can be caused by disturbances or excessive changes in the input. For that reason negative feedback promotes stability.
This leads to an error signal, which is defined by the difference between the desired setpoint and the process variable. The error signal is used by the controller to calculate a correcting force that is needed to control the plant. In many motion systems with a feedback loop, PID controllers - or variations of them - are being used. The goal of the controller is to decrease the error signal by calculating a correcting control variable. In this example, the actuator force is the control variable and that force is calculated by three separate terms: the proportional, integral and derivative.
The feedback controller thus needs an error signal to control force and this error signal arises due to the presence of a given setpoint or disturbance. The control signal is transformed to an analog signal that is useful for the plant. In motion systems, this strategy is not very favorable because feedback always reacts with a certain amount of delay. A feed forward strategy, see figure 2.11, could be a solution to this issue. When the plant model is known, the control signal can be derived from the desired motion profile. Thus the signal is being anticipated by using the characteristics of the motion system because it needs to be known how much inertia, friction and other loads can be expected to make an accurate approximation of the required control force. Nevertheless feedback is still needed since the used model of the plant cannot be perfect in practice and thus errors will arise that can only be minimised by a feedback strategy. In addition disturbances will arise that are unknown due to their nature.

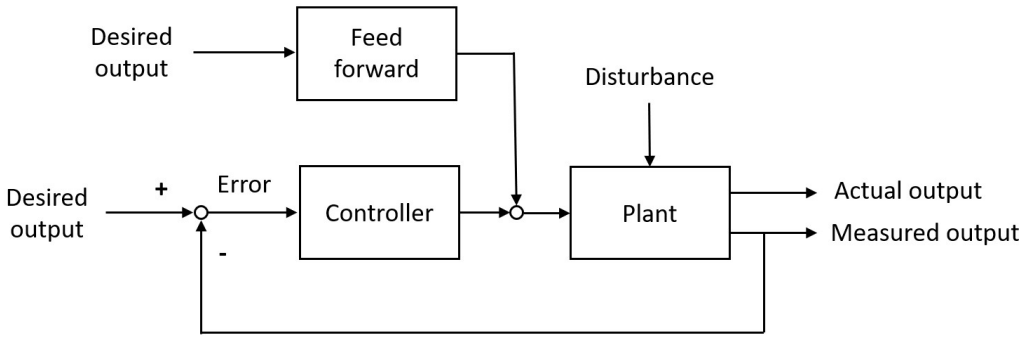

Figure 2.11: System block diagram of a typical motion system with feed forward strategy

Thus there are several controller strategies available for control systems; not only for motion systems. A relevant question that appears here is to which characteristics this control system is designed. This is largely determined by underlying goals such as oscillation damping, removing steady-state error, improving stability or speed of response. To be able to design it is necessary to analyse the dynamic characteristics and this could be done by the frequency response. An advantage of this approach is the possibility to identify the response experimentally, which is realised by applying sinusoidal input for a desired spectrum to the system and then measuring the amplitude and phase of the output. Besides experimental identification it is possible to derive the frequency response based on the mathematical model of the dynamic system. This information can be plotted in diagrams to visualise the response and offer insights to engineers working on control design.
This study focuses on motion systems, thus it is necessary to examine the frequency response of the proposed system in figure 2.10. The Bode diagram in figure 2.12 shows the relation between actuator force F and the output position of the trolley. In fact it is a transfer function. This enables to determine how much gain is needed to let the system behave in the desired manner. This relation improves at lower frequencies because that is the case of an quasi-static situation. This means that a very slowly fluctuating load at the trolley is applied thus it is reasonable that the body follows the actuator force meticulously.

However in some applications rapidly changing actuator forces are desired, for example the laser of a CD reader. This laser has to cover relatively small distances, but at high frequency to achieve sufficient reading speed. If the Bode diagram in 2.12 would be the CD reader's one, then the actual displacement of the CD

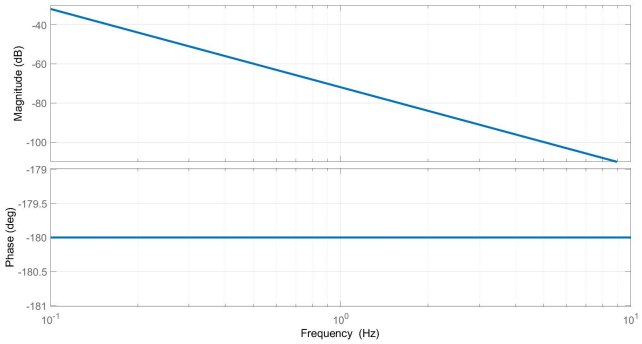

Figure 2.12: Bode diagram of transfer function from actuator force F to trolley position x of typical motion system

reader at a frequency of 1 Hz is only but a fraction of the desired one. In fact the CD reader will almost not move.
Controllers offer the solution to this problem. By using the correct actions it becomes possible to achieve required performance in the desired *bandwidth*.
Bandwidth is defined as the range from 0 Hz until the unity-gain cross-over frequency, where the amplitude of the open-loop frequency response exceeds a value of one [16].
Therefore the desired maximum operating frequency must be determined. For the CD reader, this means the maximum frequency at which the system must move in order to achieve the required reading speed. With this information, the required gains of the P, I and D actions are determined and when these gains are applied by the controller the magnitude line will shift.
In addition to bandwidth, the system's *stability* is an important criterion. For the purpose of this study the Bounded Input Bounded Output (BIBO) definition of stability is used, which states that a system is stable if the output remains bounded for all bounded inputs over any amount of time. This means that the dynamic system will move to the correct position or move back to its stable equilibrium and not blow up during operation.
Stability is impaired by resonance characteristics of the system. This could be mechanical or control characteristics, but also sensor related. Control has the purpose to decrease the effect of these resonances.
The input-output relationship of dynamic systems could be represented by transfer functions. Laplace transformations are used to work more efficiently with complex systems. This is a method that converts time-based differential equations, which describe the dynamic system, into linear algebraïc equations using the Laplace parameter s as variable.
Conditions for using the Laplace transform are that the differential equations describing the system are linear and time-invariant. The Laplace parameter is a complex variable: $s = \sigma + j\omega$. The general shape of the Laplace form is a fraction of two polynoms.
Before the Laplace transform could be applied the dynamic equations have to be derived. This means that the actuator force and acceleration of the mass have to be related for the trolley and this gives:

$$m\ddot{x}(t) = F(t) \tag{2.1}$$

The Laplace transformation gives:

$$ms^2x(s) = F(s) \tag{2.2}$$

Now the transfer function between actuator force F and trolley position x is determined:

$$\frac{x(s)}{F(s)} = \frac{1}{ms^2} \tag{2.3}$$

The roots of the numerator of equation 2.3 are called zero's and the roots of the denominator are called poles. Mathematically speaking, stability means that for a system to be stable all the poles of its transfer function must lie in the left half of the complex plane. The solution of the transfer function consist of a real and imaginary part. The real solution determines the response speed and the imaginary part determines the response frequency (oscillation) of the system.
The Bode diagram, for example figure 2.13, is used to assess stability and performance of a closed-loop system

by observing its open-loop behavior. If at the phase crossover frequency the corresponding magnitude of the transfer function is less than 0 dB, then the unity feedback system is stable. Two quantities, gain margin and phase margin, can be used to indicate the margin the system has before it goes unstable. The gain margin is the required open-loop gain to make the closed-loop system unstable and is measured at the phase crossover frequency, thus where the open-loop system's phase equals -180 degrees. Gain margin indicates endurance against changes in system parameters before the closed-loop becomes unstable. For example, the mass of a positioning machine changes when cargo is released or flexibilities in the mechanism change due to wear. All these factors influence system dynamics as can be seen by measuring the gain margin. The phase margin is the required open-loop phase shift to make the closed-loop system unstable and is measured at the gain crossover frequency, thus were the open-loop system's gain equals 0 dB. Phase margin measures the system's tolerance to time delay. Phase margin also indicates whether there is sufficient phase lag to add filters to the system.

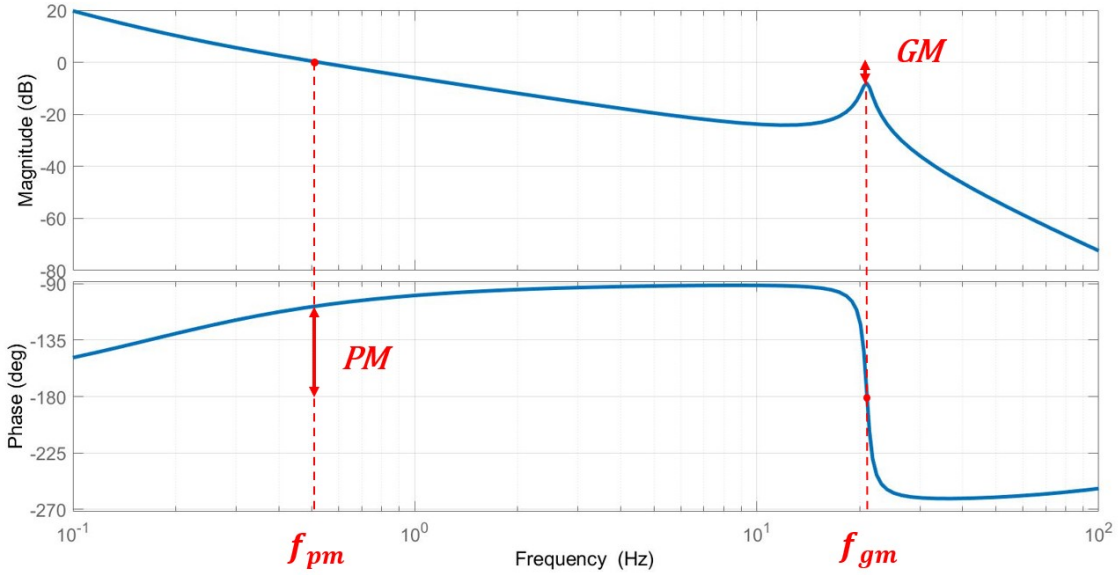

Figure 2.13: Bode diagram of the open-loop transfer function of a typical motion system with PD control showing the gain and phase margins and corresponding crossover frequencies. This system has a gain margin of 8 dB and a phase margin of 72 degrees which indicate sufficient stability margin

A concept related to this is robustness. High stability margins means high robustness since the system is less sensitive to variations, uncertainties and imperfections. This is pursued because designed systems could behave different in reality because of wrong assumptions, never obtaining perfect models or other factors. Especially in heavy equipment robustness is an important criterion because the machinery operates in proximity of human workers. The level of required margin is dependent on the application and regulations.

2.3.2. Identified dynamic effects

The second order system as considered in figure 2.10 hardly endures machine dynamics regarding bandwidth and stability, but more realistic motion systems do encounter drawbacks due to flexibilities in their construction. These flexibilities cause mechanical resonances and this will limit the bandwidth and stability. The influence of these flexibilities could be minimised by proper design, but it will not undo them. Furthermore controller strategies can be used to solve resonance issues, but this brings additional difficulties which is not always desired.
During system evaluation of the MCC concepts two flexibilities have been identified that could degrade performance. Figure 2.14 shows the location of these flexibilities in an overview of the crane vessel.

- **Actuator flexibility**

The connection between powertrain and end-effector passes several parts in many motion systems and the connections between these parts all contain flexibility. See Appendix A.1 and A.2 for a more detailed description of the parts of the actuator types used in the MCC. Due to the compliance between drive system and load the system has own dynamics and will not act like one rigid body. These connections can be modelled by lumped element modelling; spring and damper elements represent stiffness and damping properties. By investigating serial and parallel configurations, parts can be reduced to one element and their equivalent property has to be calculated. For the mass block, transmission ratio's and inertia of parts must be considered as well because equivalent mass represents the additional load that is experienced by the motor or drive to move the original load.

- **Crane boom flexibility**
  The motion system is attached to the crane boom which has limited flexibility and should not be considered as a rigid frame. Thus the crane boom will move when reaction forces are exerted at the crane tip due to motion system operation. This brings additional disturbances that have to be compensated, but this is difficult to realise because a control strategy is required that is able to track the displacement of the crane boom and react to do that on top of the disturbances arising from the vessel motion. This study attempt to investigate and quantify the influence of crane boom flexibility on motion compensation performance and how it affects the feasibility of the MCC.

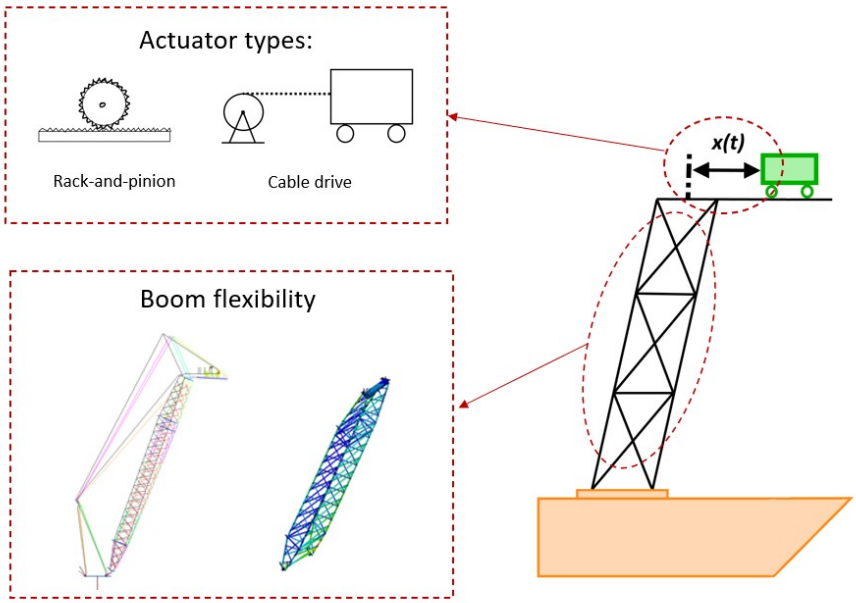

Figure 2.14: Overview of the crane vessel showing the locations of two parts that bear flexibility and are therefore of interest for further study regarding their dynamic behavior and its influence on the motion compensation performance

2.3.3. Input disturbance

To design the MCC in a proper way it is necessary to know the influence of endured disturbances because this is the first goal of the system: compensating undesired motion. The displacement transmissibility is useful to investigate this influence since it displays the system's capability to transmit motion, both inside a body as well as between bodies. Here vessel disturbances are projected at and transmitted through the crane boom and compensation mechanism to the trolley. Due to the flexible connections between these parts and flexibility of the parts itself, the magnitude of the actual disturbance at the tip will not be equal to the input disturbance.
Displacement transmissibility is very relevant in sensitive equipment such as microscope heads [16]. The microscope has to stay focused at the object, as can be seen in figure 2.15, but this is complicated by base

disturbances x_b such as floor vibrations. When disturbances act on the machine frame they will be transmitted to the microscope, but since the connection between frame and microscope is not infinitely rigid and the head has inertia, the microscope head will not follow accelerations perfectly which will cause an alignment error x_e with the object. It is key to limit this error to an acceptable level in order to make the microscope fulfill the performance requirements.

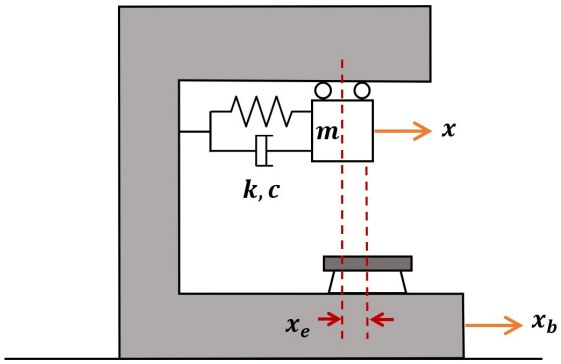

Figure 2.15: Overview of the microscope head that experiences displacement transmissibility from base disturbances. Due to limited stiffness and damping and mass of the microscope head, it will not be able to perfectly track the object. Figure adapted from [16]

The displacement transmissibility thus shows a ratio between the amplitude of base and mass motions which essentially is a transfer from displacement to displacement. This transfer is relevant for the amount of disturbance that occurs in the system and will therefore be included in the system block diagram.
To investigate the influence of displacement transmissibility the transfer of motion has to be calculated. This is possible for the microscope head from figure 2.15 by determining its equations of motion. The sum of all forces acting on the body by the spring, the damper and acceleration should be zero. The force equation is influenced by the relative displacement between frame and body because this will create force in the spring and damper element. Acceleration in the positive x-direction gives a reaction force in the opposite direction and movement of the microscope head in the same direction will induce force in the positive x-direction. Now the force equation can be written to:

$$m\ddot{x}(t) = c(\dot{x}_b(t) - \dot{x}(t)) + k(x_b(t) - x(t)) \tag{2.4}$$

Shifting terms and applying the Laplace transformation results in:

$$(ms^2 + cs + k)x(s) = (cs + k)x_b(s) \tag{2.5}$$

Rewrite to transfer function form:

$$\frac{x(s)}{x_b(s)} = \frac{cs + k}{ms^2 + cs + k} \tag{2.6}$$

The effects of displacement transmissibility can be displayed in Bode diagrams, as is done for the system of figure 2.15 in figure 2.16

For very low frequencies the numerator equals the denominator and the transmissibility will be one. This is similar to a system that moves infinitely slow thus it becomes likely that this behavior will occur. The s term in the numerator, which is related to the damper, increases the transmissibility proportional with frequency depending on the damping ratio. With the damping ratio defined as $zeta = \frac{c}{2\sqrt{km}}$.
The s term of the damper in the numerator decreases the beneficial effect of transmission reduction at higher frequencies because without this term the transmissibility would only be determined by the denominator with a s^2 term causing a -2 slope in the magnitude response.
The natural frequency of the system is determined by the stiffness and mass of the body and can be calculated by $\omega_0 = \sqrt{\frac{k}{m}}$. Damping reduces the resonance peak at the natural frequency. However, for higher frequencies

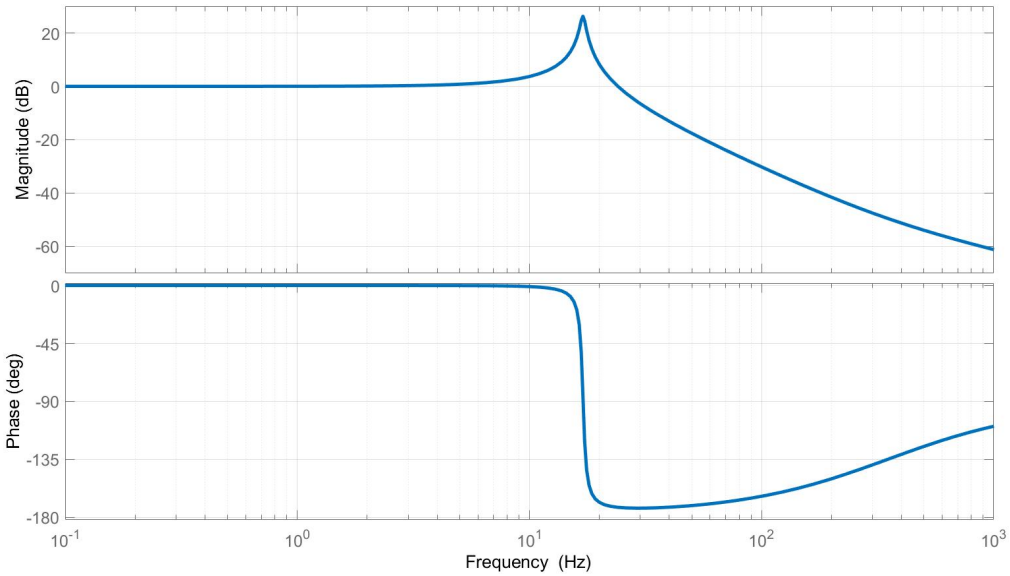

Figure 2.16: Bode diagram of the displacement transmissibility transfer function from base motion x_b to output motion x

the amplification from base to body is increased because a stronger damper gives a stronger connection between the supporting frame and the body. For motion compensation systems it is key to minimise the effects when the system is excited near its natural frequency.

3

System modelling

To be able to decide whether the proposed concepts are feasible, the feasibility criteria should be assessed with the available design specification. In order to fulfill this objective, challenges must overcome because system assessment is only possible if the control and plant are specified to a certain degree while this is not naturally since the design process is at an early stage. This is disadvantageous because among other things control theory requires a certain degree of design specification in order to design a controller. This is realised by identifying parameters of the current conceptual designs.
First the plant model of the MCC is investigated. The correct approximation of reality is determined with attention for model simplification to prevent that the model already becomes unnecessary complicated. After that the controller is designed, the controller strategy and its parameters are identified. Then the method to assess the system for realistic offshore conditions is described. Finally the model is verified with Simscape to identify errors and to highlight the usability of Simscape because it is a powerful tool to model complex systems.

3.1. Plant dynamics

The designer of motion systems is confronted with several questions about how rigid the system will be, what the positioning accuracy of the system will be and whether there will be disturbing dynamic effects. Actually the conceptual design stage is crucial to arrange the interaction between such issues and the integration of the subsystems and the design of these systems and its components. Choices made at this stage have major consequences for the remainder of the design process, including design of other systems. In order to realise an integrated design two challenges must overcome: sufficient specifications such that the controller can be designed and a definitive model of the plant [18] [19]. These challenges also appear in this study and its feasibility assessment task because information about the plant and controller is needed too. This section treats the characterisation of the plant dynamics. It is key to keep the model simple and at a low order to make it possible for engineers to interpret the model easily and to easily relate the plant properties to the properties of the motion system components. In addition this gives reliable estimations of the dominant dynamic behavior and reliable interpretations of the behavior of the controlled system later on.
The plant model thus has to be a simplification of reality, but it may not degrade the accuracy of results to much. For now a better question is which behavior must the model represent. For motion systems the stiffness of its parts and connections between these parts is very relevant. A system with a very high stiffness compared with the servo stiffness (the gain in the position loop) will not be influenced by mechanical elasticity. In that case the system can be described as a second order system. Second order motion systems do not have theoretically limit in achievable positioning accuracy as long as the servo stiffness can be increased. In practice there are limits due to the finite bandwidth of (electronic) components, their saturation level and non-linearities. In this study these conditions will not be taken into account [20].
But if mechanical elasticity does have influence on the dynamic behavior of the system, then the motion system must be described by a higher order system. By hand fourth order systems - which have one flexibility - could be treated well. Higher order systems are, however, significantly more difficult, especially regarding control design, and could therefore better be modelled and analysed by software tools.

In reality motion systems have much higher orders because they consist of interconnected component models, such as models of mechanisms, actuators, amplifiers and guidances. The resulting model thus contains multiple transmissions and many parameters, as can be seen in figure 3.1. This also brings multiple eigenmodes and corresponding natural frequencies, which will influence system dynamics and its performance.

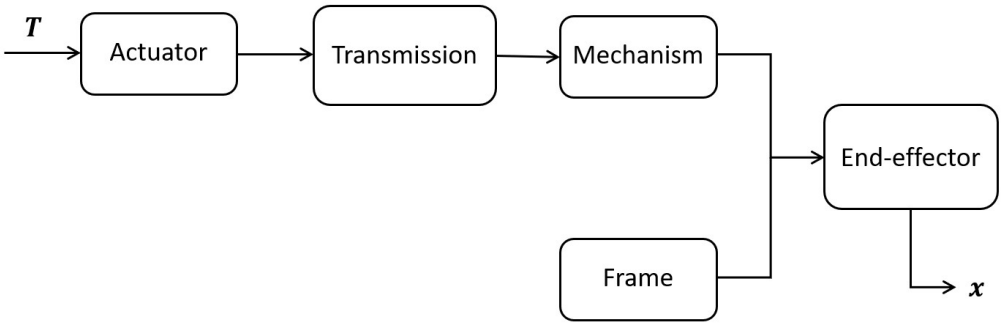

Figure 3.1: Model of the interconnected components of the positioning table system. Input motor torque T to output position x

For engineers the lowest mode of vibration is relevant and this motivates to apply model reduction. Model reduction changes both the representation and content of plant models to remove higher-order effects. It is useful to reduce to the fourth order because this will results in a simple and interpretable model consisting a small number of parameters. Yet it describes the performance-limiting factor well and is therefore a good basis to provide reliable estimates of the system behavior.
Up until now the most simplified representation of the MCC is the second order model, see figure 2.10. The conditions of this model are that one motion direction is described. All motions are transformed to translations while in reality the MCC is a combination of translating and rotating systems. In fact the actuator force is a motor with gearbox that rewritten to force by using transmission ratio's. Friction or viscous damping is not considered as well as stiffness.
The next step in model reduction is the description of the motion system in a two degrees of freedom (DOF) model. The degrees of freedom are the motion of the actuator and the motion of the end-effector, namely the trolley. With this approach it is possible to take into account the dynamic properties of the driven mechanism because the movements of the input member (actuator) and output member (end-effector) are distinguished and can be described separately.

3.1.1. Plant and actuator type

Now it is possible to investigate the influence of the actuator type by modelling its flexibility. The configuration in figure 3.2 represents the moving mechanism part of the MCC. The actuator force F is applied to the first body with mass m_{eq} that is coupled to the second body with mass m_t by the spring with stiffness k and damper with damping c. Here the body with mass m_{eq} can be seen as the total equivalent inertia at the load. The motor 'feels' this additional load on top of the trolley mass m_t when it is in operation. The spring and damper term represent the actuator flexibility that is an equivalent property of the connections between the components of the motion system. Both the equivalent mass, stiffness and damping will be calculated in Section A.1 and Section A.2. Another important aspect that was not included in figure 2.10 is the crane tip displacement x_d. This represents the input disturbance of the dynamic system.

The plant transfer function from the input force F to the output trolley position X_t is derived because this is relevant for the system dynamics and used for controller design. Therefore the balance of forces acting on both bodies according to the second law of Newton is derived. Body with mass m_{eq}:

$$m_{eq}\ddot{x}_m(t) = F(t) + c\,(\dot{x}_t(t) - \dot{x}_m(t)) + k\,(x_t(t) - x_m(t)) \tag{3.1}$$

And body with mass m_t:

$$m_t\ddot{x}_t(t) = -c\,(\dot{x}_t(t) - \dot{x}_m(t)) - k\,(x_t(t) - x_m(t)) \tag{3.2}$$

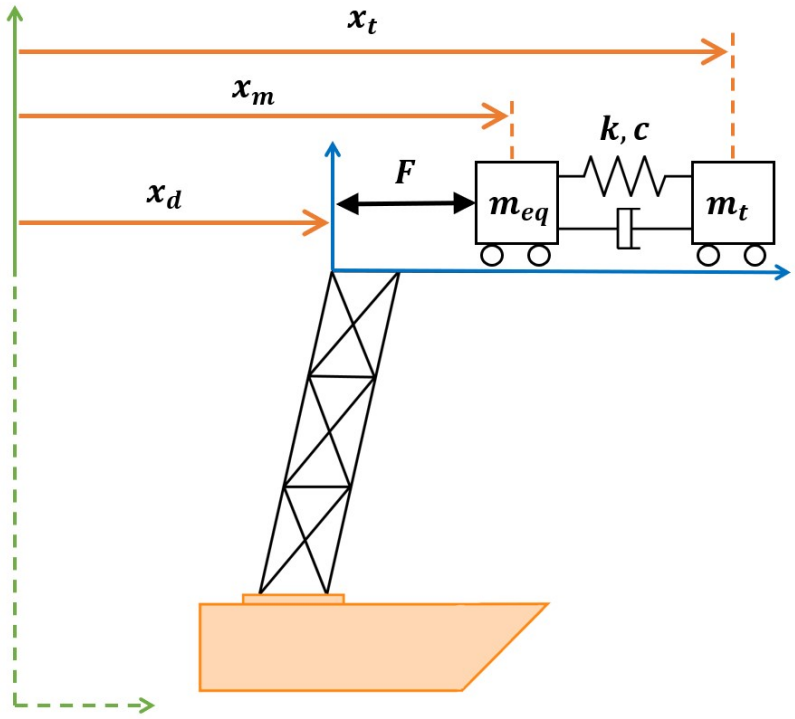

Figure 3.2: Lumped element model of the motion system located at the crane tip. Orange arrows denote the system's DOF, green arrows the world frame and blue arrows the crane tip frame

After applying the Laplace transformation the equations are written as follows:

$$\left(m_{eq}s^2 + cs + k\right) x_m(s) = F(s) + (cs + k)x_t(s) - (cs + k)x_d(s) \tag{3.3}$$

$$\left(m_t s^2 + cs + k\right) x_t(s) = (cs + k)x_m(s) + (cs + k)x_d(s) \tag{3.4}$$

Which can be written into the following transfer of F to x_t, denoted G_1:

$$G_1(s) = \frac{-(k + cs)}{(k + cs)^2 - \left(m_t s^2 + cs + k\right)\left(m_{eq}s^2 + cs + k\right)} \tag{3.5}$$

Next the values of the system parameters are identified. These values are dependent on the actuator type. Parameters of the rack-and-pinion system are derived in Appendix A.1. Parameters of the cable system are derived in Appendix A.2. An overview of the used components can be found in Appendix A.1 and A.2.
When equation 3.5 is re-arranged to obtain a form where a multiplication of factors is used, the multiplicative expression for the transfer function G_1 in the Laplace domain becomes:

$$G_1(s) = \frac{1}{\left(m_{eq} + m_t\right)s^2} \cdot (cs + k) \cdot \frac{1}{m_c s^2 + cs + k} \tag{3.6}$$

With the combined mass term:

$$m_c = \frac{m_{eq}m_t}{m_{eq} + mt} \tag{3.7}$$

The system has three natural frequencies. Two of them correspond to both a double pair of poles of the system:

$$p_{1,2} = 0 \tag{3.8}$$

$$p_{3,4} = \frac{-c \pm \sqrt{c^2 - 4m_c k}}{2m_c} \tag{3.9}$$

And the other corresponds to one zero of the system, which gives an anti-resonance frequency:

$$z_1 = -\frac{k}{c} \tag{3.10}$$

This explains the behavior in frequency domain, see figure 3.3. Interesting is that trends at low and high frequencies are similar for both actuator types. The characterising difference is described by the second pair of poles in equation 3.9. This is the natural frequency that is valuable for controller design and it is obvious that this frequency is strongly dependent on the values of the system parameters and thus directly related to design choices.

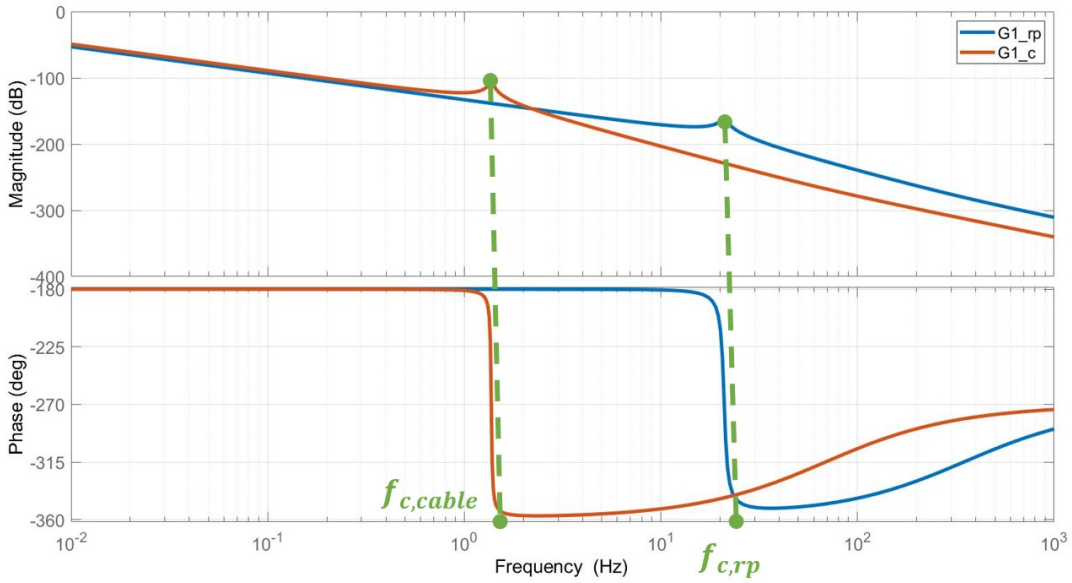

Figure 3.3: Bode diagram of the transfer function from plant actuator force F to trolley output position x_t. Both actuator types and their natural frequencies are represented

3.1.2. Displacement transmissibility

The current lumped element model is not able to represent, however, an important characteristic correctly; the displacement transmissibility. In the model the connection between input disturbance and trolley is not useful because the actuator force cannot transmit displacement while this is an important feature within motion compensation systems. A solution is making use of the lever mechanism, as shown in figure 3.4. The lever mechanism is a graphical representation that makes it clear that the system contains an additional DOF and it couples the disturbance and actuator displacement to trolley position. It makes it possible to deal with the situation when the crane tip starts moving, but the actuator is not controlled yet. This is explained in the following steps:

1. Disturbance motion propagates and frame starts moving.
2. Trolley feels acceleration, force acts on trolley, trolley starts pulling at (flexible) drive connection.
3. Force builds up in drive connection (the spring-damper element).
4. Results in small deflection; motor part of drive rotates small amount, so x_m, while there is no active control. This is the resulting trolley motion due to disturbance

To understand how the dynamics change after using the lever representation the EOM have to be rewritten. Consider the original EOM as described in equations 3.1 and 3.2. Movements of the end-effector m_t

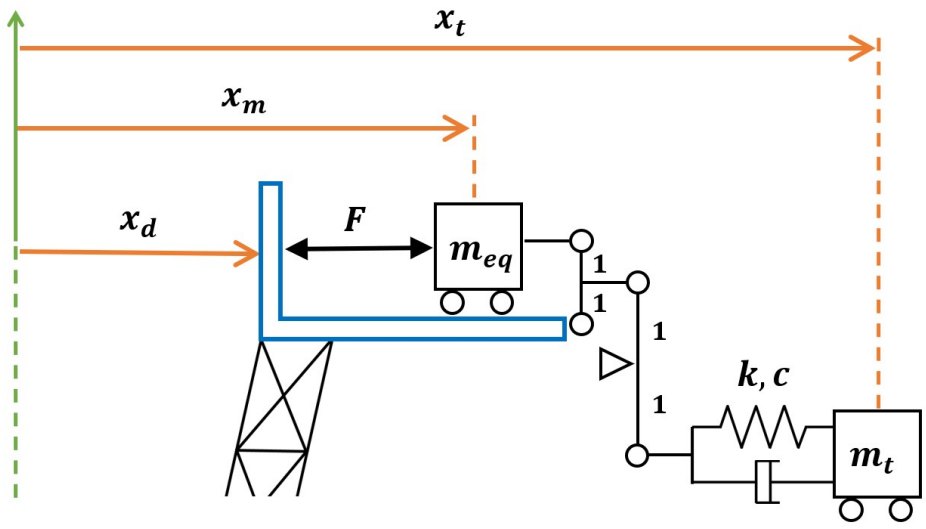

Figure 3.4: Lever representation of the MCS and lumped element model showing the coupling of disturbance and actuator displacement to trolley position. The arms of the lever have equal lengths. Orange arrows denote the system's DOF, green arrows the world frame and blue lining the crane tip frame

are now a combination of movements due to actuator displacement and frame vibrations. Thus the EOM become:

$$m_{eq}\ddot{x}_m(t) = F(t) + c\left(\dot{x}_t(t) - \dot{x}_m(t) - \dot{x}_d(t)\right) + k\left(x_t(t) - x_m(t) - x_d(t)\right) \tag{3.11}$$

$$m_t\ddot{x}_t(t) = -c\left(\dot{x}_t(t) - \dot{x}_m(t) - \dot{x}_d(t)\right) - k\left(x_t(t) - x_m(t) - x_d(t)\right) \tag{3.12}$$

The plant transfer function F to x_t does not change with respect to the system as in figure 3.2. Compare with equation 3.5

$$G_1(s) = \frac{x_t(s)}{F(s)} = \frac{-(k+cs)}{(k+cs)^2 - \left(m_t s^2 + cs + k\right)\left(m_{eq} s^2 + cs + k\right)} \tag{3.13}$$

The displacement transmissibility transfer function from x_d to x_t is given by:

$$G_2(s) = \frac{x_t(s)}{x_d(s)} = \frac{m_{eq} s^2 (k+cs)}{(k+cs)^2 - \left(m_t s^2 + cs + k\right)\left(m_{eq} s^2 + cs + k\right)} \tag{3.14}$$

There is no one-to-one transmissibility; this is visible in the frequency response of the transfer function in figure 3.5. There is an offset for small frequencies. This relates to the situation where the platform starts moving. Then the trolley on top tends to roll slightly, but inertia needs to accelerate, and then it starts following the platform.

3.1.3. Crane boom flexibility

Another influence on the plant dynamics - because of its flexibility - is situated in the crane boom, which forms the coupling between vessel and compensation system. Therefore the motion compensation performance could be reduced because the crane boom moves when the compensation system is under operation and exerts forces at the crane tip that can generate additional disturbances.
For modelling purposes it is again key to determine the lowest natural frequency since this is the largest threat to the control bandwidth. This motivates to use only one extra DOF and simplify the crane boom flexibility to one mass-spring-damper element because higher eigenmodes are irrelevant at this point. Now it is important to calculate the effective mass, damping and stiffness as perceived at the chosen physical DOF.
To introduce crane boom flexibility in the model, the diagram of figure 3.4 is extended to the diagram of figure 3.6. Note that there are now two disturbance sources that could induce crane tip displacement. These

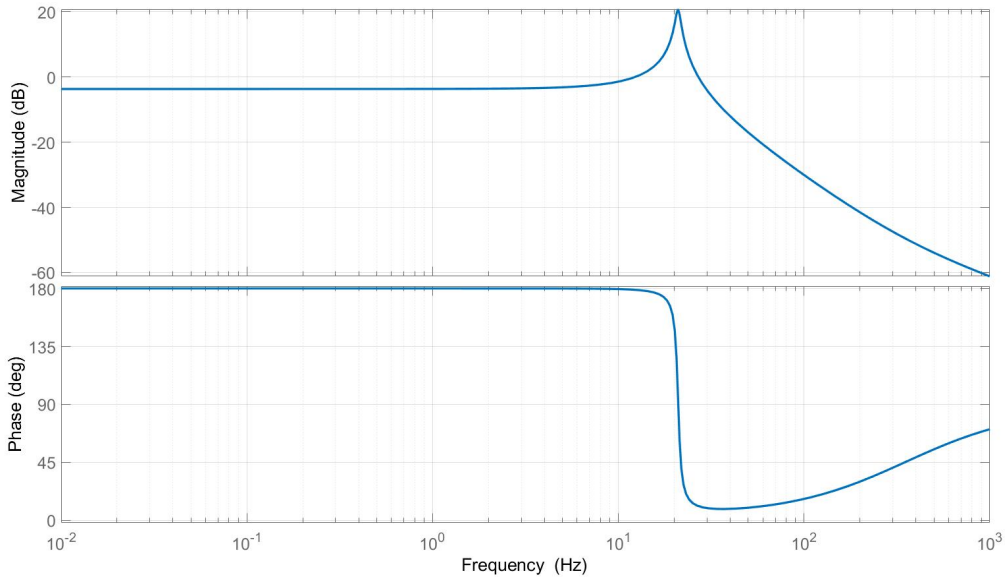

Figure 3.5: Bode diagram of the displacement transmissibility transfer function from crane tip disturbance x_d to trolley position x_t of the MCS represented in figure 3.4

DOF correspond to the movement of the vessel and crane boom. The EOM are extended with an additional equation for the crane boom mass:

$$m_{boom}\ddot{x}_d(t) = -F(t) - c_{boom}\left(\dot{x}_d(t) - \dot{x}_{d,v}(t)\right) + k_{boom}\left(x_d(t) - x_{d,v}(t)\right) \tag{3.15}$$

Note that $x_d(t) = x_{d,b}(t) + x_{d,v}(t)$. Because of this additional equation the transfer functions for the plant system and displacement transmissibility become more complicated. Its full derivation can be found in Appendix B.1 and B.2. To be able to further analyse the system and add control to create a working model of the motion system, first the parameters of the crane boom mass, damping and stiffness must be determined.
To determine one effective mass, it is assumed that the boom rotates as a rigid beam around the pivot. The effective mass is dependent on the crane boom inertia, its movement direction and the distance between crane tip and crane boom base, which is located at the boom pivot. The crane boom inertia is calculated in Appendix C.1.
The MCS moves in horizontal direction, thus the properties of the crane boom element are also transformed to horizontal direction and calculated.
The effective stiffness is determined by the stiffness of the boom hoist and the boom configuration. The calculation of the boom hoist stiffness is done in Appendix C.2.
The effective damping is determined by the boom mass, boom configuration and effective stiffness. The calculation is done in Appendix C.3.
The boom configuration thus has an influence on all boom parameters and this has consequences for the natural frequencies of the crane boom. With the found parameters it is possible to determine the frequency response of the transfer function from input force F to output trolley position x_t. For the rack-and-pinion system this is illustrated in figure 3.7.
Note that the crane boom flexibility generates a resonance in combination with anti-resonance in the plant transfer function. More interesting is the fact that the frequencies are closer to the required control bandwidth than the natural frequency of the actuator flexibility. This means that there is more risk that crane boom flexibility will degrade motion compensation performance.
Also the frequency response of the transfer function from vessel disturbance $x_{d,v}$ to output trolley position x_t is determined. For the rack-and-pinion system this is illustrated in figure 3.8. Again the crane boom flexibility causes a resonance frequency that is closer to the control bandwidth.

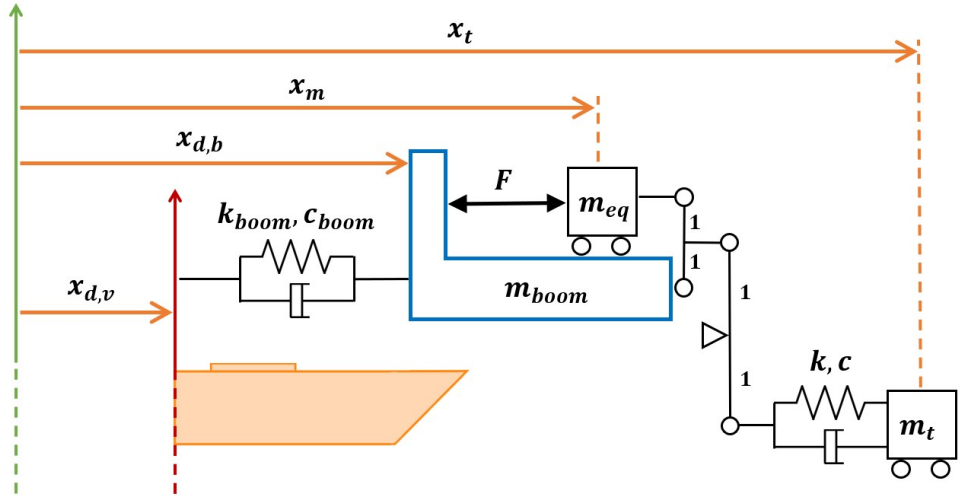

Figure 3.6: Lever representation of the MCC and lumped element model including the crane boom flexbility. Orange arrows denote the system's DOF, green arrows the world frame, blue lining the crane tip frame and red arrows the vessel frame

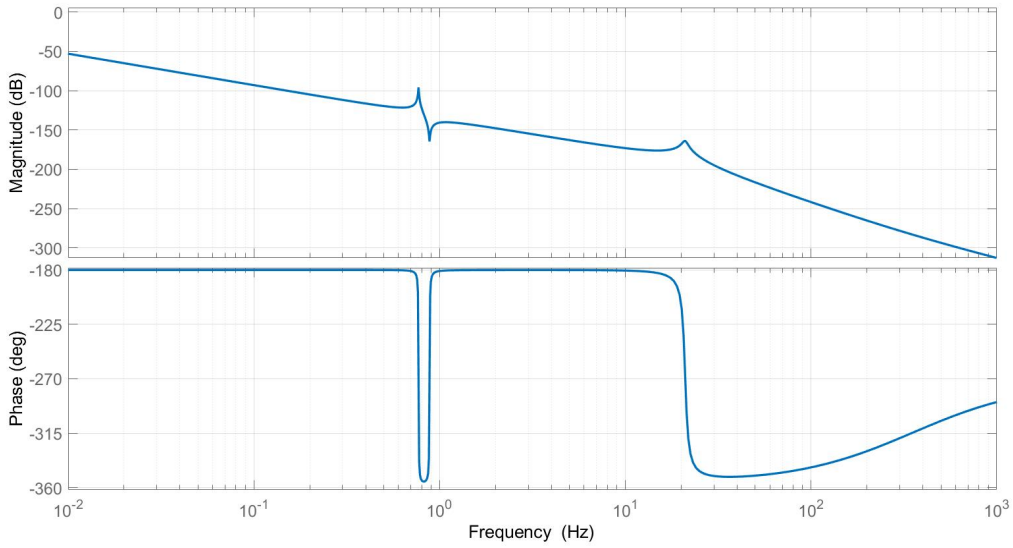

Figure 3.7: Bode diagram of the plant transfer function from actuator force F to trolley position x_t of MCC with crane boom flexibility

3.2. Control design

The controller of the MCS controls the plant and ensures that the desired behavior is obtained as good as possible. The goal of motion compensation is disturbance rejection and this motivate to use the block diagram in figure 3.9 as the control loop. In this feedback control strategy the control action is based on the difference between the desired motion, the r signal, and the actual motion, signal x_t. For motion compensation purposes it is necessary to keep the system at a certain point and for that reason $r = 0$ is chosen.

Another important difference with the typical feedback control diagram of figure 2.9 is the presence of the displacement transmissibility transfer function. This represents the relation between input disturbance and output trolley position, against which the compensator must react. The outcome of this displacement transmissibility is independent on the controller and plant dynamics. Without active control this would thus

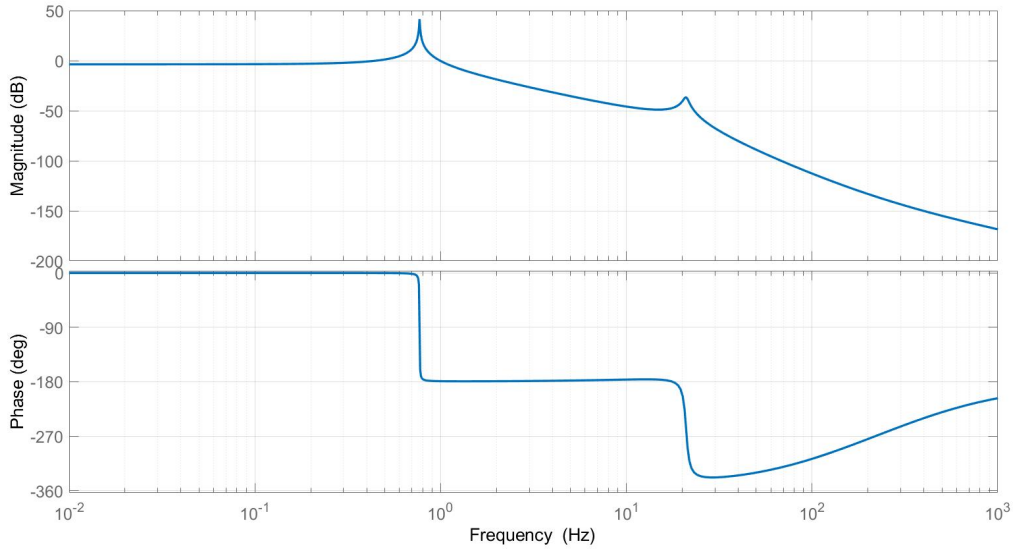

Figure 3.8: Bode diagram of the displacement transmissibility transfer function from vessel disturbance $x_{d,v}$ to trolley position x_t of MCC with crane boom flexibility

show how the trolley moves purely because of acting disturbances. The output of the plant and displacement transmissibility transfer function are summed and thus form the output trolley signal.
The control loop used in this model uses position signals. Regarding model complexity this is easier to design and it has practical benefits since trolley deviation with respect to the reference point is well interpretable and relatable to OWT installation requirements.
Feedback control allows to stabilise marginally stable or unstable systems and is therefore useful in motion systems [16]. To realise this, the sensor signal is fed back in a closed-loop to the input of the system, which is r in the case of this study. For this reason, feedback control is also called closed-loop control and its transfer functions are used to investigate the system's performance. The control system in figure 3.9 has two of these closed-loop transfer functions, namely T and H:

$$x_t = \frac{G_1(s)C(s)}{1+G_1(s)C(s)}r + \frac{G_2(s)}{1+G_1(s)C(s)}x_d \tag{3.16}$$

$$T(s) = \frac{x_t}{r} = \frac{G_1(s)C(s)}{1+G_1(s)C(s)} \tag{3.17}$$

$$H(s) = \frac{x_t}{x_d} = \frac{G_2(s)}{1+G_1(s)C(s)}x_d \tag{3.18}$$

T shows the reference tracking capability and H shows the disturbance rejection capability. Thus H is the most relevant performance indicator for motion compensation systems.
From figure 3.9 it becomes apparent that the connection of the various blocks determines the final system performance. Normally the controller block is the one that engineers could design the most freely and thus rely on the most to improve the performance. In this study the controller is designed by using the frequency response of the open-loop system. How the sinusoidal output changes as a function of frequency is a useful indicator of the system's time response. In addition the system's frequency response is important to determine the robustness of the system. Here two quantities are being used, gain margin and phase margin to indicate the margin the system has before it goes unstable. The MCS is required to have 6 dB of gain margin and 60 degrees of phase margin. These stability margins are a valuable method to determine the overall stability of the closed-loop system from the open-loop design.

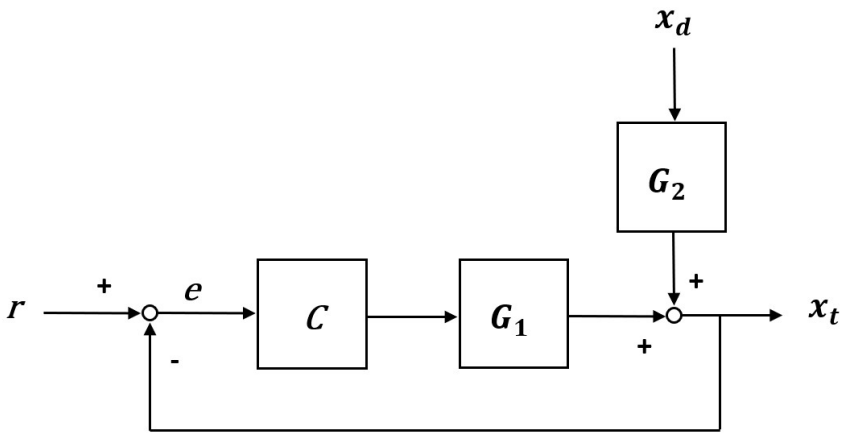

Figure 3.9: System block diagram used in this study to control the MCS

3.2.1. Controller design for rack-and-pinion system

The open-loop transfer functions $L(j\omega)$ of the plant with several controller strategies (PD, PID, with/without tamed action) are evaluated on basis of frequency response. Outcomes show that the PD strategy fulfills the margin requirements well for the rack-and-pinion system when standard tuning guidelines are maintained. The system has a gain margin of 8 dB, phase margin of 72 degrees and bandwidth of 0.52 Hz.

$$L(s) = C_{pd}(s)G_1(s) \tag{3.19}$$

$$C_{pd}(s) = K_p + K_d s \tag{3.20}$$

$$K_t = |G_1(\omega_c)| \tag{3.21}$$

$$K_p = \frac{K_t}{3} \tag{3.22}$$

$$K_d = \frac{3K_p}{\omega_c} \tag{3.23}$$

This allows to tune the proportional and derivative parameters K_p and K_d to increase the bandwidth until the controller just meets the margin requirements. The reason to do this is that the performance improves as can be seen in figure 3.10. This is especially visible at low frequencies; higher magnitude means better response to the error signal, which is the input of the controller. Eventually the bandwidth increases to 0.72 Hz.

The magnitude response of the closed-loop disturbance rejection transfer function H is shown in figure 3.11. Low magnitude indicates good disturbance rejection. Especially the magnitude in the region below the bandwidth frequency should be as low as possible. The diagram also shows the magnitude response of the displacement transmissibility transfer function G_2 to verify how much the performance improves when active control is implemented.

3.2.2. Controller design for cable system

Furthermore the controller of the cable system has to be designed. Recall that the resonance frequency caused by actuator flexibility is closer to the bandwidth for the cable system with respect to the rack-and-pinion system. When the same strategy for controller selection and design is maintained, it appears that the cable system does not achieve the required gain margin. Two solutions will be investigated.
The first one makes use of notch filters. Notch filters have an inverse characteristic of the resonating eigenmode to suppress this specific resonance by pole-zero cancellation [16]. The notch shape thus resembles an

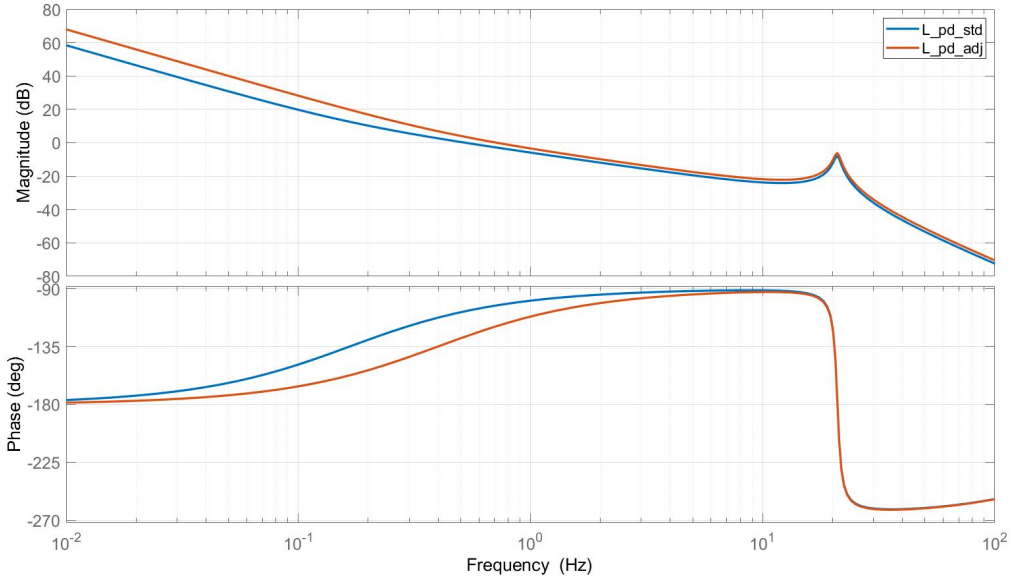

Figure 3.10: Bode diagram of the open-loop transfer function from input error signal e to output trolley position x_t. Blue indicates the controller with standard tuning settings and red indicates the controller with maximised bandwidth

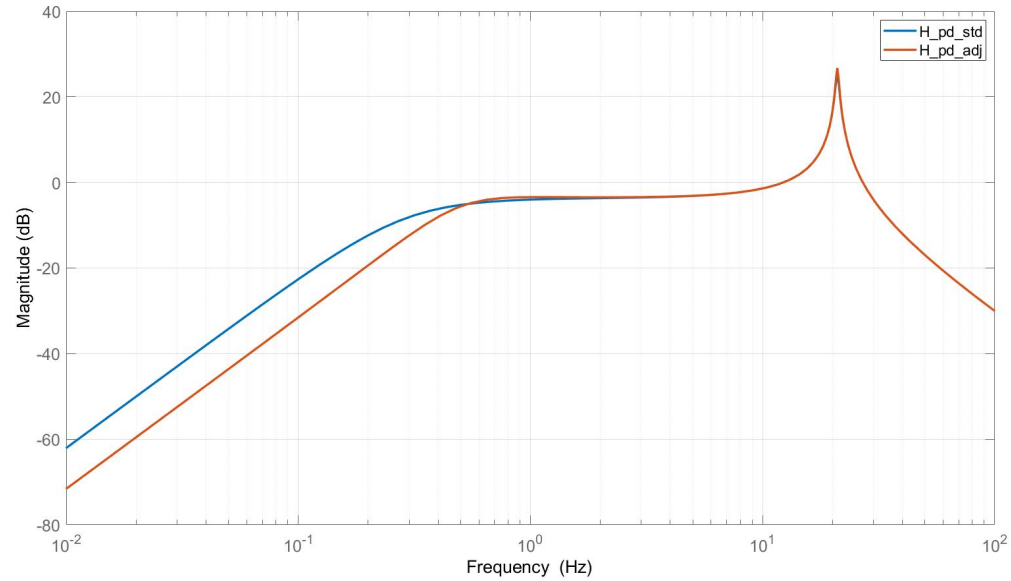

Figure 3.11: Magnitude response of the closed-loop transfer function H from input crane tip disturbance x_d to output trolley position x_t. It clearly shows the difference in performance at low frequencies between the standard tuned controller and controller with maximised bandwidth

anti-resonance that is used to minimise the resonance peak of the actuator flexibility. Therefore the notch filter is placed in series with the controller and plant.
The disadvantage of this method is the sensitivity to parameter variations and inaccuracies. The method requires an almost perfect tuning of the frequency and damping ratio parameter, particularly when the resonance shows a very high Q-factor, and this is difficult to achieve because of the spread in system dynamics of the controller, plant and other system components.
In addition the application of notch filters costs phase margin. If well tuned it will cost about 30 degrees of

phase margin, but this is still to much to achieve the stability margin. However now the gain margin requirement is achieved.
The robustness problem of the notch filter could be solved by soft notch. This means that the filter is applied to a broader frequency band by choosing a different ratio between the damping factors of the pole and zero part. But the soft notch filter costs even more phase margin and this makes the method unsuitable for this application finally.
The other solution is to the tune the controller for a lower bandwidth. This means that the closed-loop performances such as disturbance rejection will degrade in a certain frequency range, but stability margins are being sufficed and some robustness counts more than performance in favour of the risk for instability. The eventual disturbance rejection capability does not have to be unsatisfactory since it is also dependent on the vessel-crane interaction and the wave response dynamics. This could have favourable influence. These characteristics are considered in Section 3.3.

3.2.3. Controller design for rack-and-pinion system with crane boom flexibility

Analysis of the plant transfer function shows that the resonance in combination with the anti-resonance arises close to the required bandwidth and this sets demands to the controller design strategy. In order to guarantee stability the controller is tuned for a lower bandwidth, also because it is difficult to tune a robust notch/anti-notch filter.
Only a controller for the rack-and-pinion system is designed because this suffices to investigate the research objective regarding the influence of crane boom flexibility.

3.3. Realistic offshore conditions

Another aspect that affects the performance is the operational environment of the MCC. Therefore actual conditions that cause disturbances for the MCC must be taken into account to obtain a realistic feasibility assessment. This gives a more reliable impression of the actual motion compensation performance. To do this, the relative performance is investigated, which considers the relation between waves and trolley motion in the frequency domain. Furthermore the absolute performance is considered, which determines the significant response of trolley motion to compare the trolley motion with OWT installation requirements that were derived in Section 2.1.2.
Thus both aspects are regarded. Relative performance because it is convenient for overviews on performances and its possibility to model and assess many different situations relatively fast. On top of that it is less sample-like than absolute performance which describes in the time domain. Time domain analysis has the benefit of describing the response at a high level of detail.
To determine the magnitude and direction of disturbances arising from sea waves in a certain operating point - like the crane tip - the vessel response amplitude operator (RAO) is used. The RAO is a transfer function that relates wave amplitude to 1 DOF rigid body motion, for example the heave motion of the vessel. If the phase difference between waves and vessel motion is irrelevant the absolute value can be used to express the displacement. It is possible to derive the RAO for all kinds of offshore structures and it is being used by shipbuilders to improve features such as safety or performance.
In addition to the frequency dependency of the RAO, it is also heading dependent. Heading is the wave direction towards the vessel. For workability studies it is useful to make a polar diagram in order to quickly see the most potent heading.
The response energy that is experienced at the operating point is determined by the RAO and the wave energy spectrum [21]. Such response spectra are thus calculated for the DOF defined by the RAO. This is useful because in reality an irregular wave pattern is experienced. It is not interesting to know the wave amplitude at a certain time, it is much more interesting to know the statistical properties - in terms of frequency and amplitude - of the wave behavior.
First the energy spectrum of the response is determined for the most sensitive direction at the crane tip. This direction is chosen because it is the most difficult test for the MCS to disturbances. Several parameters are needed to determine the energy response: wave spectra that act on the vessel, the frequency range of the operation and the RAO from vessel COG to crane tip.
The chosen wave spectra are Joint North Sea Wave Project (JONSWAP) type because the MCC will operate at the North Sea. The analysis is performed for four peak periods (6, 8, 10, 12 s) and three significant wave

heights (1, 2, 3 m) to investigate how performance change for various conditions. Figure 3.12 shows the energy spectrum of the waves for varying peak periods and significant wave height of 1 meter.

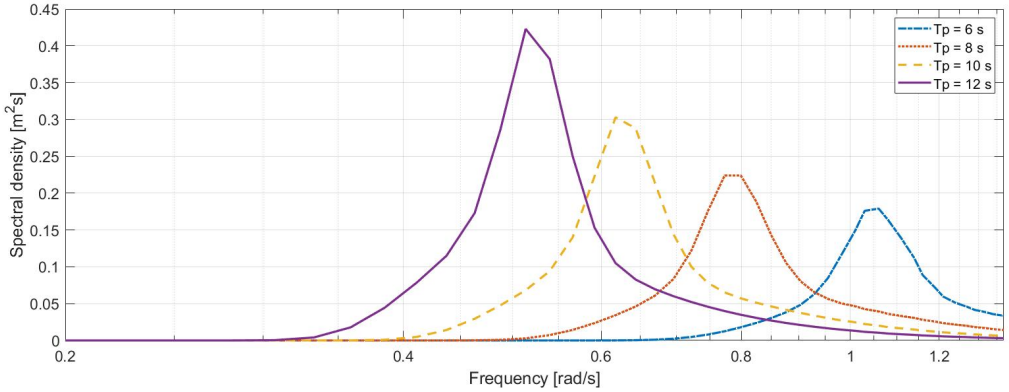

Figure 3.12: Energy spectrum of waves that are chosen as conditions for disturbance input of the studied crane vessel and MCC

The RAO's are dependent on the crane configuration and wave heading. The chosen crane configuration, $\alpha = 90$ degrees and $\beta = 71$ degrees, is useful for OWT installation and service tasks and illustrated in figure 3.13. A wave heading of 30 degrees is chosen because the vessel is most sensitive to waves in that direction.

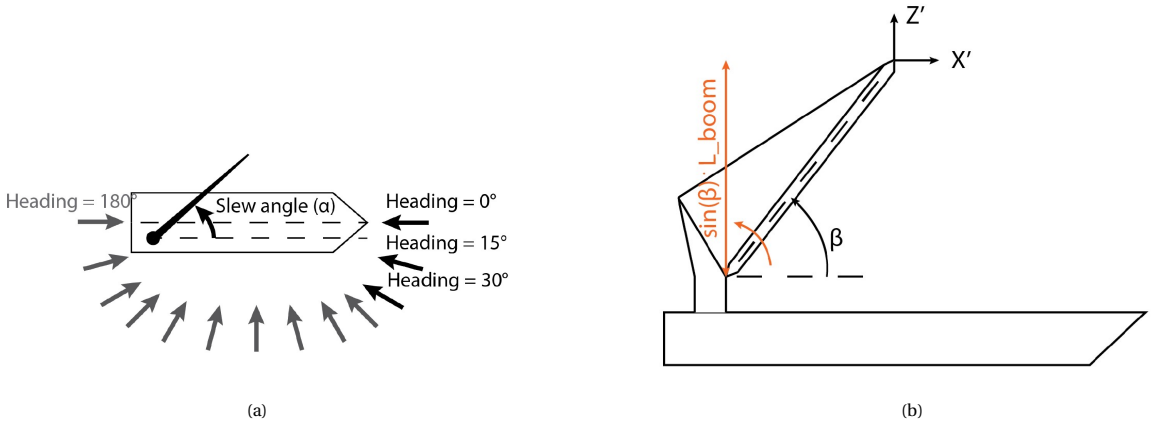

(a) (b)

Figure 3.13: Illustrations showing several conventions. Both adapted from [6] (a): Vessel headings and slewing position (b): Luffing position and local axis system at crane tip

The energy response at the crane tip for the chosen direction is calculated by the following equation:

$$S_\zeta \cdot |RAO|^2 = S_{\text{response}} \tag{3.24}$$

Note that the response scales linearly with significant wave height.

The energy spectrum of the trolley motion is determined by using the crane tip energy spectrum as input and the magnitude response of the closed-loop disturbance rejection transfer function H as transfer function. The resulting spectrum in figure 3.14 shows how realistic disturbances are being compensated.

Then time domain analysis is performed by calculating the zero-th order spectral moment m_0 of the motion spectrum by equation 3.25. With these moments the significant motion response amplitude is calculated by equation 3.26, which is defined as the 'mean value of the highest $\frac{1}{3}$th part of the amplitudes'. This is a useful value because it gives an indication of the expected disturbance behavior while working at sea. This is done for the MCC when in operation and for the same crane vessel without working MCC. Results are shown

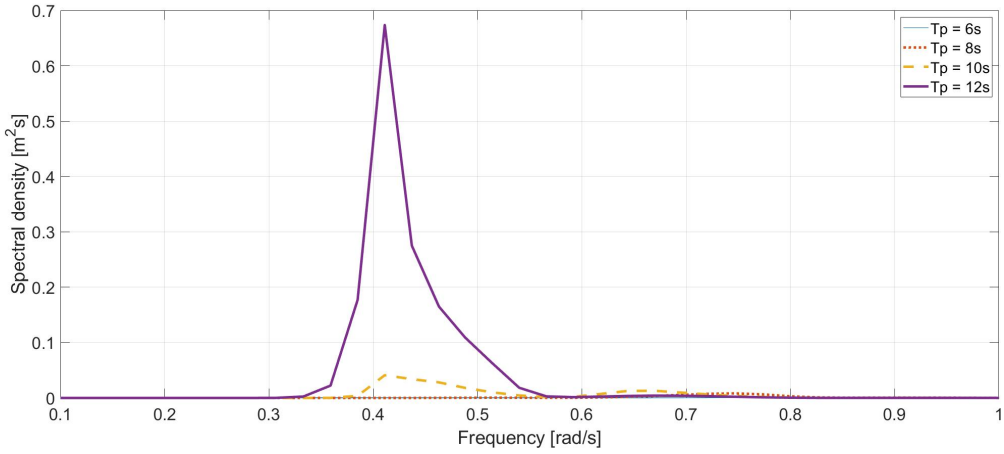

Figure 3.14: Energy spectrum of trolley motion for varying peak periods showing how well disturbances arising from sea waves are compensated by the crane vessel and MCC

and discussed in Section 4.3.

$$m_{n\zeta} = \int_0^\infty \omega^n \cdot S_\zeta(\omega) \cdot d\omega \tag{3.25}$$

$$H_{1/3} = 4 \cdot \sqrt{m_{0\zeta}} \tag{3.26}$$

3.4. Simscape verification

The Matlab based Simulink extension Simscape makes it possible to model dynamic systems in a visual way and this is used to check on analytical models for errors. In addition Simscape, or similar software, is extremely useful when more complex systems (higher order or multi-physical domain) have to be modelled. In those situations setting up an analytical model is to time-consuming and prone to errors.
Simscape builds a simulation model based on physical modelling, which relies on differential equations and energy flows to describe the behavior of the system. It provides the user with graphical modeling elements that represent physical components from various domains, such as pneumatic valves, electric motors and mechanical gears. Herewith multi-domain effects could be integrated relatively easy in the system design because no elaborate skill of mathematically describing components and integrating them is needed. Subsequently Simscape numerically solves the resulting system of differential equations. Furthermore it allows to model signals and discrete events by a port-based approach, which is useful because simplified models of system components from an early design stage can later on be replaced with more detailed models. One disadvantage here is that the multi-physics model is still based on assumptions about the expected behavior, thus significant experience is needed to obtain reliable assumptions.
Due to this approach it is also possible to combine Simscape with Simulink, build control loops and design control systems. This saves considerable time with respect to the transfer function approach that is used by analytical modelling.
Two model variations are verified: the rack-and-pinion system with and without crane boom flexibility. This is because the graphical representation of the rack-and-pinion and cable system are the same, they only have different parameter values. Thus it is unnecessary to verify both actuator types.
The model of the system without crane boom flexibility can be found in Appendix D First the plant and displacement transmissibility frequency responses are compared, then the open-loop and closed-loop responses. No differences are found.
But the model with crane boom flexibility does show differences. Its model can be found in Appendix D. Differences appear in both the plant and displacement transmissibility response and logically in the open-loop and closed-loop response, as can be seen in figure 3.15. Differences are in the order of $\frac{1}{10} Hz$ regarding natural frequencies and in the order of 5 dB regarding magnitude peaks. Note that the trend of the response is the same, there is only a small difference in frequency and peak magnitude between analytical and Simscape

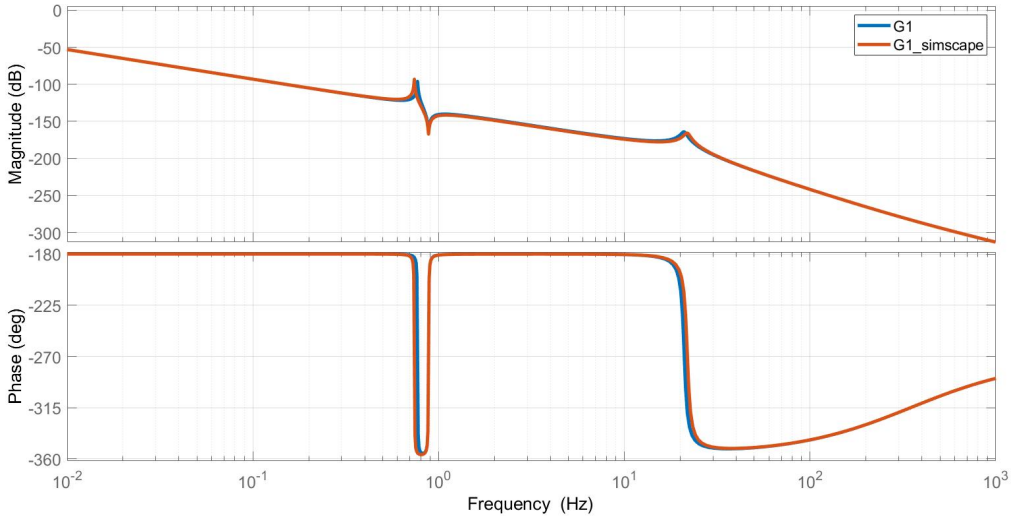

Figure 3.15: Bode diagrams of the plant transfer function showing differences between analytical and Simscape model

model.

4

Results

This chapter treats the found results related to the objectives of this study. There are three objectives:

1. Compare the performance of MCC with different actuator types to investigate the influence of actuator flexibility and dynamics.

2. Investigate the influence of crane boom flexibility.

3. Quantify the performance of the MCC for realistic offshore conditions to check whether the operational requirements of OWT installation and service activities are fulfilled.

4.1. Influence of actuator type

- The bandwidth of the cable drive system (0.02 Hz) is much smaller than the initial bandwidth specification (0.50 Hz) in order to achieve the required stability margins of 6 dB gain margin and 60 degrees phase margin. This is clearly visible in figure 4.1 at the points where the magnitude response of H bends and stops rising. More important is that this indicates the significant worse disturbance rejection capability of the cable system in the bandwidth region. Only testing for realistic offshore conditions could offer an outcome for the cable system.

- Resonance frequency of cable drive system is lower than rack-pin because of rope properties, while mass trolley of cable system is slightly lower. Thus better disturbance damping at low frequencies which is indicated by the difference between the blue and red line.

- Resonance peak of cable system is higher because of worse damping due to rope stiffness and length.

- For cable system, situation is tensive regarding performance. This could be solved by applying notch and low-pass filters, however these filters bear robustness issues.

4.2. Influence of crane boom flexibility

- Crane boom flexibility degrades bandwidth considerable: note the points in figure 4.2 where the magnitude response of H bends and stops rising.

- This problem already arises in open-loop because actuator 'senses' the flexibility of the crane boom. Thus resonance/anti-resonance arises around 0.8 Hz. It is possible to filter this, but very difficult to realise a robust filter. In closed-loop transfer function H the displacement transmissibility returns thus the effect of crane boom flexibility cannot be removed completely by filtering.

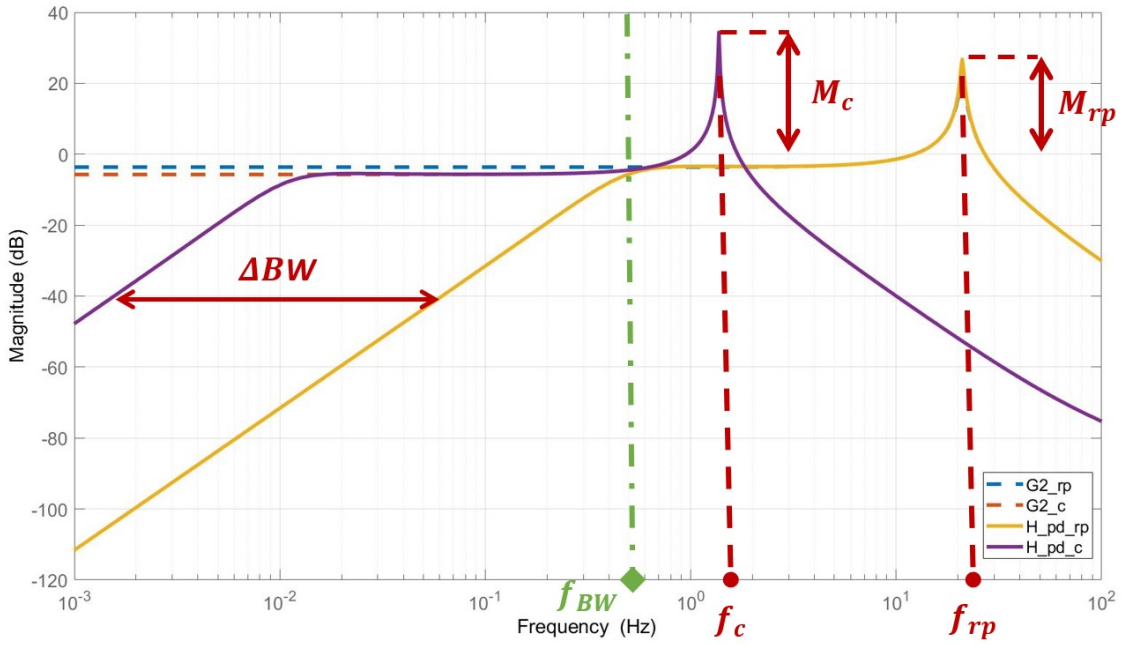

Figure 4.1: Bode diagram of closed-loop transfer function H from input disturbance x_d to output trolley position x_t and displacement transmissibility transfer function G_2 from input disturbance x_d to output trolley position x_t. Both actuation principles. Rigid crane boom configuration

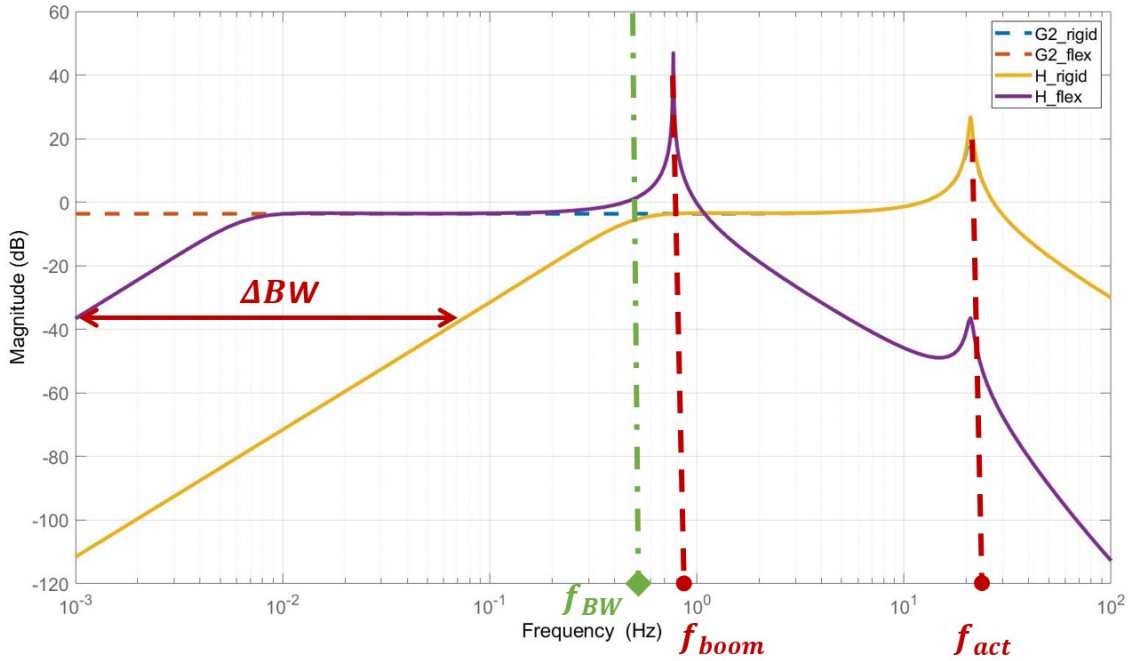

Figure 4.2: Bode diagram of the closed-loop transfer function from input disturbance x_d to output trolley position x_t. Rack-and-pinion system. Compare rigid and flexible crane boom configuration. Displacement transmissibility transfer function G_2 from input disturbance x_d to output trolley position x_t plotted as baseline

4.3. Performance in offshore conditions

Table 4.1 shows the significant output motion heights for several peak periods and significant wave heights of the trolley to indicate the workability. Values are compared relatively with the same vessel but without MCC

in operation to show how much improvement is realised by the MCC.

- It becomes clear that an increase in significant wave height leads to a less than proportional increase in significant output motion height.
- When the values in Table 4.1 are compared with the requirements for OWT installation than it is obvious that installation activities are very difficult to fulfill in most conditions. Recall that the tolerance for blade alignment is in the order of several centimeters.
- Remarkable is the more aggressive response to longer waves (higher peak periods), while the MCS performs better at those frequencies as can be seen in figure 4.2 for example. The reason for that is the increased sensitivity to waves of the vessel in that region.

	Tp = 6s	8s	10s	12s
Hs = 1m	0.027 (-32%)	0.068 (-33%)	0.145 (-33%)	0.390 (-34%)
2m	0.037 (-32%)	0.096 (-33%)	0.205 (-33%)	0.565 (-34%)
3m	0.046 (-32%)	0.118 (-33%)	0.251 (-33%)	0.692 (-34%)

Table 4.1: Significant amplitudes [m] of trolley motion for various significant wave height and peak period conditions. Values are compared relatively with the same vessel but without MCC in operation.

5

Conclusions

At this point it is hard to predict the chances of success for the MCC. This study gives insight into the influence of actuator type, crane boom flexibility and possibilities to estimate performance for offshore conditions. The method is developed, but for definite feasibility conclusions many more situations and conditions have to be investigated.
The following remarkable findings resulted from this study:

- Robustness appears to be a major issue. It endangers stability, especially for the flexible crane boom configuration.
- The lever representation is a good method to overcome the shortcoming of the lumped element model to include displacement transmissibility in systems with flexible base-frame structures.
- Simscape is a valuable tool to model complex (mechanical) systems and check analytical models for errors. It can also be used for multi-domain systems which is a major benefit for mechatronic system design. Sound integration of multiple (sub)system models is made much easier.
- Section 4.1 hows that it is dangerous to choose an actuator type with a low natural frequency because it degrades performance. From equation 3.9 it appears that the frequency is determined by several parameters, but in general it applies that actuator types with higher stiffness will have an higher natural frequency and are therefore more suitable.
- In Section 4.3 it becomes evident that MCC operation gives a significant improvement of performance. This improvement is almost constant for the various offshore conditions that have been tested.

6

Recommendations

Some parts were considered to be outside the scope of this study. Other parts have been found during the study and invite to perform further research:

- Investigate other aspects that could influence the performance of the MCC, such as power and force limitations, delays and uncertainties. Quantify their influence on the performance.
- Implement the control strategy with combined feedback and feed forward. Thus feed forward for main disturbance rejection and feedback for correction and anti-drifting. By doing this the model will represent the real system better. It is also useful to examine if the performance will improve by adding feed forward control.
- Perform a full workability analysis by simulating more scenarios regarding offshore conditions and vessel and boom configurations.
- Compare performance of the MCC with conventional jack-up vessels.
- Elaborate the performance test for offshore conditions. Now only significant height is considered. Suitability of other performance indicators that relate to OWT installation requirements should be investigated.
- Elaborate the performance test for more boom configurations and other DOF. It is important to quantify the sensitivity of the system to various configurations.
- Improve identification of plant, actuator dynamics and flexibilities such as crane boom. Now only the most simplified parameters are used, but it has not been verified how much accuracy is lost by this approach. If well motivated and only if advantages surpass the modelling complexity, other components could be added to the model as well but realise more identification is needed.
- Continue research on how stability margins are endangered by system properties such as flexibilities. Investigate which control methods can be used to improve performance regarding these aspects.
- Develop a model of the hoist ropes, hook-yoke assembly and tuggers to assess the performance of the MCC with payload swing. This aspect was idealised in this study.
- Identify the performance limiting factors in the current model and investigate whether the influence of these factors is realistic. Come up with approaches to improve the performance either by mechanical design or control methods.
- Assess the reliability and accuracy of the used models with respect to realistic predictions. Suggest how reliability and accuracy could be improved such as more detailed modelling and simulation or by practical verification methods such as experiments.

Bibliography

[1] A. S. Verma, Z. Y. Jiang, Z. R. Ren, Z. Gao, and N. P. Vedvik, "Response-based assessment of operational limits for mating blades on monopile-type offshore wind turbines," *Energies*, vol. 12, no. 10, p. 26, 2019, ISSN: 1996-1073. DOI: 10.3390/en12101867.

[2] D. Ahn, S.-c. Shin, S.-y. Kim, H. Kharoufi, and H.-c. Kim, "Comparative evaluation of different offshore wind turbine installation vessels for korean westsouth wind farm," *International Journal of Naval Architecture and Ocean Engineering*, vol. 9, no. 1, pp. 45–54, 2017, ISSN: 2092-6782. DOI: https://doi.org/10.1016/j.ijnaoe.2016.07.004.

[3] O. ; Huisman, "Maintenance of large offshore wind turbine generators - 3d motion compensation," Report, 2020.

[4] Huisman, "Huisman equipment internal document," Report, 2021.

[5] Z. Gao, W. Guachamin, L. Li, Y. Zhao, C. Li, and T. Moan, "Numerical simulation of marine operations and prediction of operability using response-based criteria with an application to installation of offshore wind turbine support structures," 2016.

[6] J. Buijs, "3d motion compensation - develop a design method," Report, 2017.

[7] Y. Zhao, "Numerical modeling and dynamic analysis of offshore wind turbine blade installation," 2019. [Online]. Available: http://hdl.handle.net/11250/2611272.

[8] M. P. J. Driessen, "Feasibility assessment of motion compensated cranes: A literature study," Report, 2021.

[9] L. Kuijken, "Single blade installation for large wind turbines in extreme wind conditions," Thesis, 2015.

[10] Web Page. [Online]. Available: https://liftra.com/product/lifting-yoke-for-blades/.

[11] Figure, 2012. [Online]. Available: http://www.siemens.com/presspictures/copyright.

[12] Z. Y. Jiang, Z. Gao, Z. R. Ren, Y. Li, and L. Duan, "A parametric study on the final blade installation process for monopile wind turbines under rough environmental conditions," *Engineering Structures*, vol. 172, pp. 1042–1056, 2018, ISSN: 0141-0296. DOI: 10.1016/j.engstruct.2018.04.078.

[13] A. S. Verma, Z. Y. Jiang, N. P. Vedvik, Z. Gao, and Z. R. Ren, "Impact assessment of a wind turbine blade root during an offshore mating process," *Engineering Structures*, vol. 180, pp. 205–222, 2019. DOI: 10.1016/j.engstruct.2018.11.012.

[14] Web Page. [Online]. Available: https://www.ge.com/renewableenergy/wind-energy/offshore-wind/haliade-x-offshore-turbine.

[15] HuismanEquipment, "3d motion compensated crane - basis of design," Report, 2019.

[16] R. M. Schmidt and I. O. S. Press, *The design of high performance mechatronics : high-tech functionality by multidisciplinary system integration*, 2nd revised edition. Amsterdam: Delft University Press, 2014, ISBN: 9781614993681 1614993688.

[17] A. M. Rankers, "Machine dynamics in mechatronic systems, an engineering approach," Thesis, 1997.

[18] E. Coelingh, T. J. A. de Vries, and R. Koster, "Assessment of mechatronic system performance at an early design stage," *IEEE/ASME transactions on mechatronics*, vol. 7, no. 3, pp. 269–279, 2002, ISSN: 1083-4435.

[19] H. J. Coelingh, "Design support for motion control systems - a mechatronic approach," 2000.

[20] H. Groenhuis, "A design tool for electromechanical servo systems," Thesis, 1991.

[21] J. M. J. Journée and W. W. Massie, *Offshore Hydromechanics*, First. Delft University of Technology, 2001.

A

Actuator parameters and component specification

A.1. Rack-and-pinion system

The drive system of the rack-and-pinion is schematically represented in figure A.1:

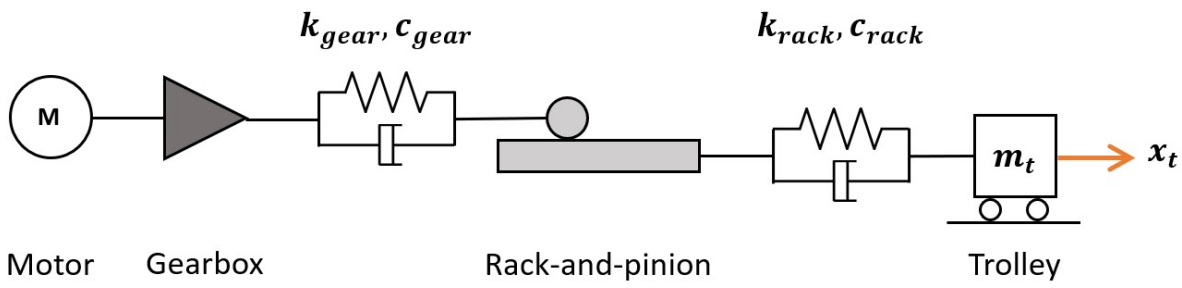

Figure A.1: Schematic diagram of the rack-and-pinion drive system

Two of such drive systems are used per motion direction. In order to calculate the equivalent mass, first the inertia of one drive system has to be determined. This is given by the following equation:

$$J_{eq} = \left(n_m J_m + n_m J_g\right) i_g^2 \tag{A.1}$$

Here n_m represents the number of electric motors, J_m the inertia of one motor, J_g the inertia of the gearbox measured at the input (motor) side and i_g the gearbox transmission ratio.

The equivalent mass with respect to all drive systems is given by:

$$m_{eq} = n_{rp} J_{eq} i_{rp}^2 \tag{A.2}$$

Here n_p is the number of drive systems, J_{eq} the inertia of one drive system and i_{rp} the geometric transmission at the pinion gear to transform the rotational motion into translation.

The influence of the stiffness of the rack-and-pinion system is dominated by the gearbox stiffness. Stiffness of the rack itself is considered to be very high and therefore it will not be taken into account in this study.

Gearbox stiffness is calculated with:

$$k_{rot} = T_2 \cdot 100 \tag{A.3}$$

Here T_2 is a gearbox constant.

Total gearbox stiffness is equal to:

$$k_{rot,tot} = n_{rp} n_m k_{rot} \tag{A.4}$$

For this model the total translational stiffness needs to be calculated, this is:

$$k_{tra,tot} = k_{rot,tot} i_{rp}^2 \tag{A.5}$$

Where i_{rp} is the geometric transmission:

$$i_{rp} = \frac{2}{D_{eff}} \tag{A.6}$$

D_{eff} is the effective diameter of the pinion gear and calculated by:

$$D_{eff} = m n_p \tag{A.7}$$

The total translation damping is dependent on the total translational stiffness and is calculated by:

$$c_{tra,tot} = 2\zeta \sqrt{k_{tra,tot} m_*} \tag{A.8}$$

Here m_* is:

$$m_* = \frac{m_{eq} m_t}{m_{eq} + mt} \tag{A.9}$$

This gives $m_{eq} = 7.47e4kg, c = 2.03e5 \frac{Ns}{m}$ and $k = 4.45e8 \frac{N}{m}$

The following parameters are used:

Component	Property	Value	Unit
Trolley			
	m_t	$39e3$	kg
Electric motor			
	J_m	4.15	$kg \cdot m^2$
	n_m	1	–
Gearbox			
	i_g	18	–
	J_g	0.1	$kg \cdot m^2$
	T_2	$82e3$	Nm
	ζ	0.03	–
Gearing			
	m	$24e-3$	m
	n_g	42	–
	n_p	16	–
	n_{rp}	2	–

A.2. Cable system

The cable drive system is schematically represented in figure A.2:

Here the stiffness and damping of the ropes that are attached to the moving parts are taken into account because they have a considerable length that will influence the dynamics. Per motion direction one drive system is used. In addition to the rack-and-pinion system the winch has inertia and another gearbox is used.

In order to calculate the rope stiffness and damping, first the rope area must be calculated:

$$A = \frac{1}{4} \pi d^2 \tag{A.10}$$

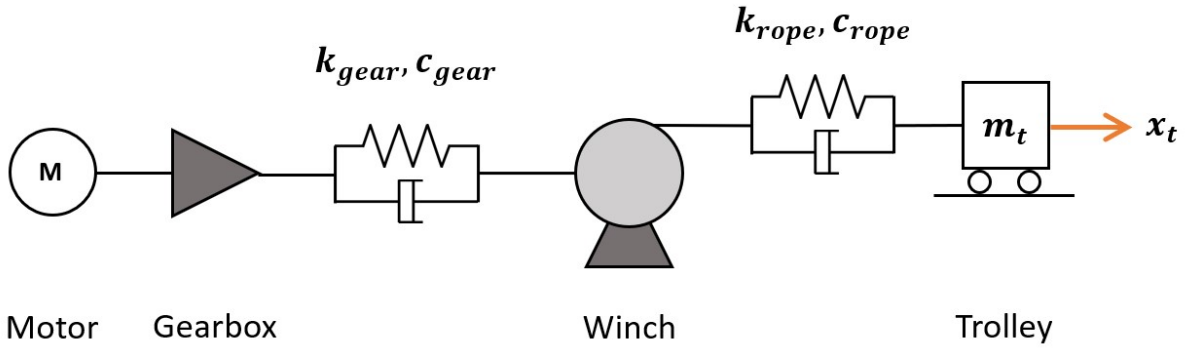

Figure A.2: Schematic diagram of the cable drive system

Now the rope stiffness can be calculated

$$k_{rope} = \frac{pt_{fac}AE}{L} \tag{A.11}$$

After that the rope damping can be calculated as well

$$c_{rope} = 2\zeta\sqrt{k_{rope}\left(\frac{J_w}{r_w^2} + \frac{1}{2}m_t\right)} \tag{A.12}$$

Due to the winch inertia, the equation to calculate the total inertia changes:

$$J_{eq} = \left(n_m J_m + n_m J_g\right) i_g^2 + J_w \tag{A.13}$$

The equivalent mass will now be calculated at the winch with the following geometric transformation:

$$n = \frac{1}{r_w} \tag{A.14}$$

Gearbox stiffness is again calculated by equation A.3.
But the total rotational gearbox stiffness is now calculated by:

$$k_{rot,tot} = k_{rot} \tag{A.15}$$

Thus the total translational gearbox stiffness is calculated by:

$$k_{tra,g} = k_{rot,tot} n^2 \tag{A.16}$$

The total translational gearbox damping is calculated by:

$$c_{tra,g} = 2\zeta\sqrt{k_{tra,g} m_*} \tag{A.17}$$

Here m_* is calculated as in equation A.9
Now the total translational stiffness and damping of the system can be calculated. Note that the rope and drive elements act in a series configuration. Thus the equation to calculate the stiffness becomes:

$$k_{tra,tot} = \frac{1}{\frac{1}{k_{rope}} + \frac{1}{k_{tra,g}}} \tag{A.18}$$

And the equation to calculate the damping:

$$c_{tra,tot} = \frac{1}{\frac{1}{c_{rope}} + \frac{1}{c_{tra,g}}} \tag{A.19}$$

This gives $m_{eq} = 3.70e4kg, c = 3.07e3\frac{Ns}{m}$ and $k = 1.33e6\frac{N}{m}$

The following parameters are used:

Component	Property	Value	Unit
Trolley			
	m_t	$34.5e3$	kg
Electric motor			
	J_m	4.15	$kg \cdot m^2$
	n_m	2	–
Gearbox			
	i_g	24	–
	J_g	0.1	$kg \cdot m^2$
	T_2	$82e3$	Nm
	ζ	0.03	–
Rope			
	d	$3.6e-2$	m
	E	$100e9$	$\frac{N}{m^2}$
	L	150	m
	$zeta_r$	0.01	–
	pt_{fac}	2	–
Winch			
	r_w	0.374	m
	J_w	280	$kg \cdot m^2$

B

Crane boom flexibility

B.1. Plant transfer function

The system in figure 3.6 has 3 EOM:

$$m_{boom}\ddot{x}_d(t) = -F(t) - c_{boom}\left(\dot{x}_d(t) - \dot{x}_{d,v}(t)\right) + k_{boom}\left(x_d(t) - x_{d,v}(t)\right) \tag{B.1}$$

$$m_{eq}\ddot{x}_m(t) = F(t) + c\left(\dot{x}_t(t) - \dot{x}_m(t) - \dot{x}_d(t)\right) + k\left(x_t(t) - x_m(t) - x_d(t)\right) \tag{B.2}$$

$$m_t\ddot{x}_t(t) = -c\left(\dot{x}_t(t) - \dot{x}_m(t) - \dot{x}_d(t)\right) - k\left(x_t(t) - x_m(t) - x_d(t)\right) \tag{B.3}$$

With the corresponding Laplace transforms:

$$\left(m_{boom}s^2 + c_{boom}s + k_{boom}\right)x_d(s) = -F(s) + (c_{boom}s + k_{boom})x_{d,v}(s) \tag{B.4}$$

$$\left(m_{eq}s^2 + cs + k\right)x_m(s) = F(s) + (cs + k)x_t(s) - (cs + k)x_d(s) \tag{B.5}$$

$$\left(m_t s^2 + cs + k\right)x_t(s) = (cs + k)x_m(s) + (cs + k)x_d(s) \tag{B.6}$$

Note that $x_d = x_{d,b} + x_{d,v}$

Simplify expressions with following constants:

$$Z_1 = m_t s^2 + cs + k \tag{B.7}$$

$$Z_2 = cs + k \tag{B.8}$$

$$Z_3 = m_{eq}s^2 + cs + k \tag{B.9}$$

$$Z_4 = c_{boom}s + k_{boom} \tag{B.10}$$

$$Z_5 = m_{boom}s^2 + c_{boom}s + k_{boom} \tag{B.11}$$

First goal is to obtain plant transfer function F to x_t. Therefore $x_{d,v} = 0$, thus $x_d = x_{d,b}$. Now rewrite equation B.6, substitute constants to simplify notation:

$$Z_1 x_t(s) = Z_2 x_m(s) + Z_2 x_{d,b}(s) \tag{B.12}$$

$$x_t(s) = \frac{Z_2}{Z_1} x_m(s) + \frac{Z_2}{Z_1} x_{d,b}(s) \tag{B.13}$$

Rewrite to obtain $x_m(s)$

$$x_m(s) = \frac{Z_1}{Z_2} x_t(s) - x_{d,b}(s) \tag{B.14}$$

Now rewrite equation B.5:

$$Z_3 x_m(s) = F(s) + Z_2 x_t(s) - Z_2 x_{d,b}(s) \tag{B.15}$$

Substitute $x_m(s)$:

$$Z_3 \frac{Z_1}{Z_2} x_t(s) - x_{d,b}(s) = F(s) + Z_2 x_t(s) - Z_2 x_{d,b}(s) \tag{B.16}$$

Rewrite:

$$(\frac{Z_3 Z_1}{Z_2} - Z_2) x_t(s) = F(s) + (Z_3 - Z_2) x_{d,b}(s) \tag{B.17}$$

Now obtain form $G_1(s) = \frac{x_t}{F}$:

$$\frac{x_t(s)}{F(s)} = \frac{1}{\frac{Z_3 Z_1}{Z_2} - Z_2} + \frac{Z_3 - Z_2}{\frac{Z_3 Z_1}{Z_2} - Z_2} \frac{x_{d,b}(s)}{F(s)} \tag{B.18}$$

Rewrite equation B.4:

$$(m_{boom} s^2 x_{d,b}(s) = -F(s) - (c_{boom} s + k_{boom}) x_{d,b}(s) \tag{B.19}$$

Rewrite to $\frac{x_{d,b(s)}}{F(s)}$:

$$\frac{x_{d,b}(s)}{F(s)} = \frac{-1}{m_{boom} s^2 + c_{boom} s + k_{boom}} = \frac{-1}{Z_5} \tag{B.20}$$

Substitute $\frac{x_{d,b(s)}}{F(s)}$ in $\frac{x_t}{F}$:

$$\frac{x_t(s)}{F(s)} = \frac{1}{\frac{Z_3 Z_1}{Z_2} - Z_2} - \frac{Z_3 - Z_2}{(\frac{Z_3 Z_1}{Z_2} - Z_2) Z_5} \tag{B.21}$$

Multiply both sides by factor $\frac{Z_2}{Z_2}$ and rewrite:

$$\frac{x_t(s)}{F(s)} = \frac{Z_2}{Z_3 Z_1 - Z_2^2} - \frac{Z_3 Z_2 - Z_2^2}{Z_3 Z_1 Z_5 - Z_2^2 Z_5} \tag{B.22}$$

B.2. Displacement transmissibility

To obtain displacement transmissibility transfer function $x_{d,v}$ to x_t, first rewrite equation B.4. Note that $F = 0$:

$$x_d(s) = \frac{c_{boom} s + k_{boom}}{m_{boom} s^2 + c_{boom} s + k_{boom}} x_{d,v}(s) = \frac{Z_4}{Z_5} x_{d,v}(s) \tag{B.23}$$

Rewrite equation B.5:

$$x_m(s) = \frac{cs + k}{m_{eq} s^2 + cs + k} x_t(s) - \frac{cs + k}{m_{eq} s^2 + cs + k} x_d(s) = \frac{Z_2}{Z_3} x_t(s) - \frac{Z_2}{Z_3} x_d(s) \tag{B.24}$$

Now substitute equation B.23 and equation B.24 in equation B.6:

$$Z_1 x_t(s) = Z_2 \left(\frac{Z_2}{Z_3} x_t(s) - \frac{Z_2 Z_4}{Z_3 Z_5} x_{d,v}(s) \right) + \frac{Z_2 Z_4}{Z_5} x_{d,v}(s) \tag{B.25}$$

Rewrite to:

$$\left(Z_1 - \frac{Z_2^2}{Z_3} \right) x_t(s) = \left(-\frac{Z_2^2 Z_4}{Z_3 Z_5} + \frac{Z_2 Z_4}{Z_5} \right) x_{d,v}(s) \tag{B.26}$$

Multiply both sides by factor $\frac{Z_3}{Z_3}$:

$$\frac{Z_1 Z_3 - Z_2^2}{Z_3} x_t(s) = \frac{Z_2 Z_4 Z_3 - Z_2^2 Z_4}{Z_3 Z_5} x_{d,v}(s) \tag{B.27}$$

Multiply both sides by factor $\frac{Z_5}{Z_5}$:

$$\frac{Z_1 Z_3 Z_5 - Z_2^2 Z_5}{Z_3 Z_5} x_t(s) = \frac{Z_2 Z_4 Z_3 - Z_2^2 Z_4}{Z_3 Z_5} x_{d,v}(s) \tag{B.28}$$

Rewrite and eliminate factor $\frac{Z_3 Z_5}{Z_3 Z_5}$:

$$\frac{x_t(s)}{x_{d,v}(s)} = \frac{Z_2 Z_4 Z_3 - Z_2^2 Z_4}{Z_1 Z_3 Z_5 - Z_5 Z_2^2} \tag{B.29}$$

C

Crane boom parameters

C.1. Effective mass

In order to find the effective mass, first the mass moment of inertia around the boom center of mass (COM) has to be determined. The COM is located at 75.23 m from the boom hinge, see figure C.1.

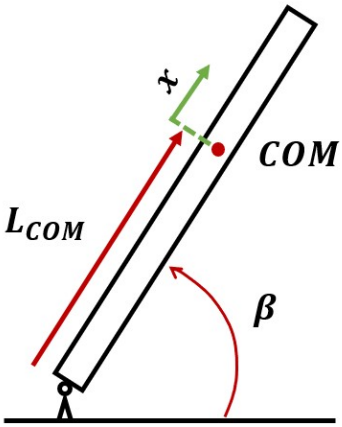

Figure C.1: Side view of crane boom with relevant lengths and parameters

To calculate the inertia, use equation:

$$I_{COM} = \frac{m_{boom}}{L_{boom}} \int_{x_1}^{x_2} \ell^2 d\ell \tag{C.1}$$

This gives $I_{COM} = 7.39e8 kg \cdot m^2$
The moment of inertia as sensed around the boom hinge is calculated by:

$$I_{boomhinge} = I_{COM} + m_{boom} x_1^2 \tag{C.2}$$

This gives $I_{boomhinge} = 3.69e9 kg \cdot m^2$
Now the effective mass as sensed at the crane tip can be calculated by:

$$m_{eff} = \frac{I_{boomhinge}}{z_{tip}^2} \tag{C.3}$$

Where:

$$z_{tip} = \sin(\beta) L_{boom} \tag{C.4}$$

This gives $m_{eff} = 313.6e3kg$

The following parameters are used:

Property	Value	Unit
m_{boom}	$521.6e3$	kg
L_{boom}	115	m
L_{COM}	75.23	m
x_1	-72.23	m
x_2	39.77	m
β	70.6	deg

C.2. Effective stiffness

To calculate the effective stiffness, use figure C.2.

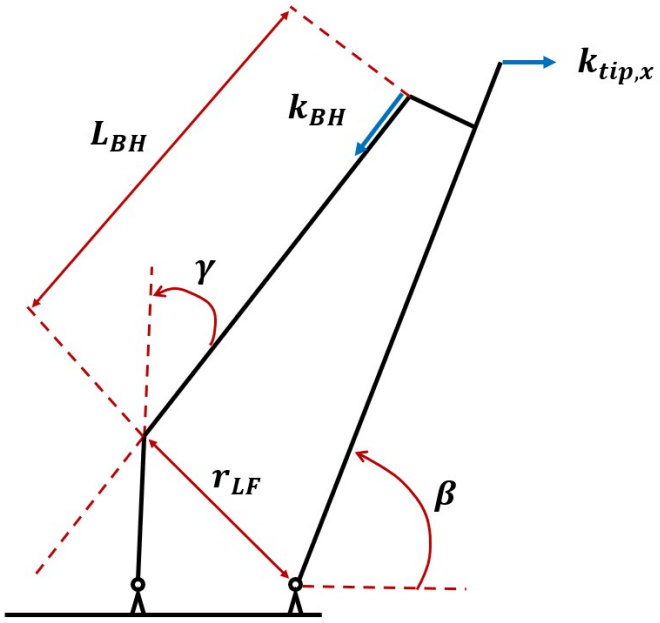

Figure C.2: Side view of crane boom with relevant lengths and parameters

The effective stiffness as sensed at the crane tip is calculated by:

$$K_{tip,x} = K_{bh} \cos\left(\gamma - 90^\circ\right) \left(\frac{r_{lf}}{r_{tip}}\right)^2 \tag{C.5}$$

Where:

$$r_{tip} = \sin\beta L_{boom} \tag{C.6}$$

The stiffness of the boom hoist is calculated by:

$$K_{bh} = \frac{N_{falls} E_{eff} A_{rope}}{L_{bh}} \tag{C.7}$$

This gives an effective stiffness of $7.34e6N/m$

The following parameters are used:

Property	Value	Unit
N_{falls}	32	–
E_{eff}	$100e9$	Pa
A_{rope}	$1.96e-3$	m^2
L_{boom}	115	m
L_{bh}	80	m
r_{lf}	43	m
β	70.6	deg
γ	48	deg

C.3. Effective damping

In order to calculate the effective damping, first the force in the boom hoist must be calculated and transformed to an equivalent mass. The force in horizontal direction is obtained from solving the moment balance around the boom pivot. Note that the boom hoist rope has to carry the load exerted by the crane boom and MCS mass:

$$F'_{bh} = \frac{\cos\theta L_1 m_{load}}{\sin\theta L_{boom}} \tag{C.8}$$

Thus:

$$F_{bh} = \frac{F'_{bh}}{\cos(\eta)} \tag{C.9}$$

Which gives the equivalent mass:

$$m_{bh} = \frac{F_{bh}}{g} \tag{C.10}$$

This gives $m_{bh} = 24.2e3kg$. Now the effective damping can be calculated:

$$c_{effective} = 2\zeta_r \sqrt{k_{rope}\frac{1}{2}m_{bh}} \tag{C.11}$$

Which results in $c_{effective} = 8.43e3\frac{N\cdot s}{m}$

The following parameters are used

Property	Value	Unit
m_{load}	$558.2e3$	kg
L_{boom}	115	m
L_1	75.23	m
η	56	deg
θ	70	deg

D

Simscape models

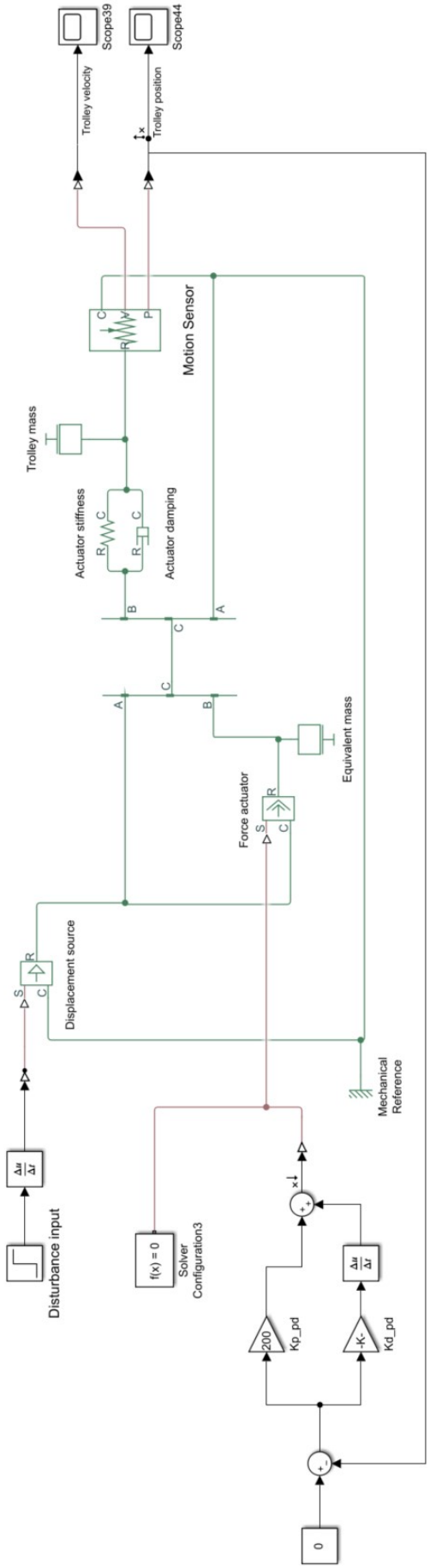

Figure D.1: Screenshot of the Simscape model with rigid crane boom showing all mechanical components, controller blocks, sensors, connections and signal wirings

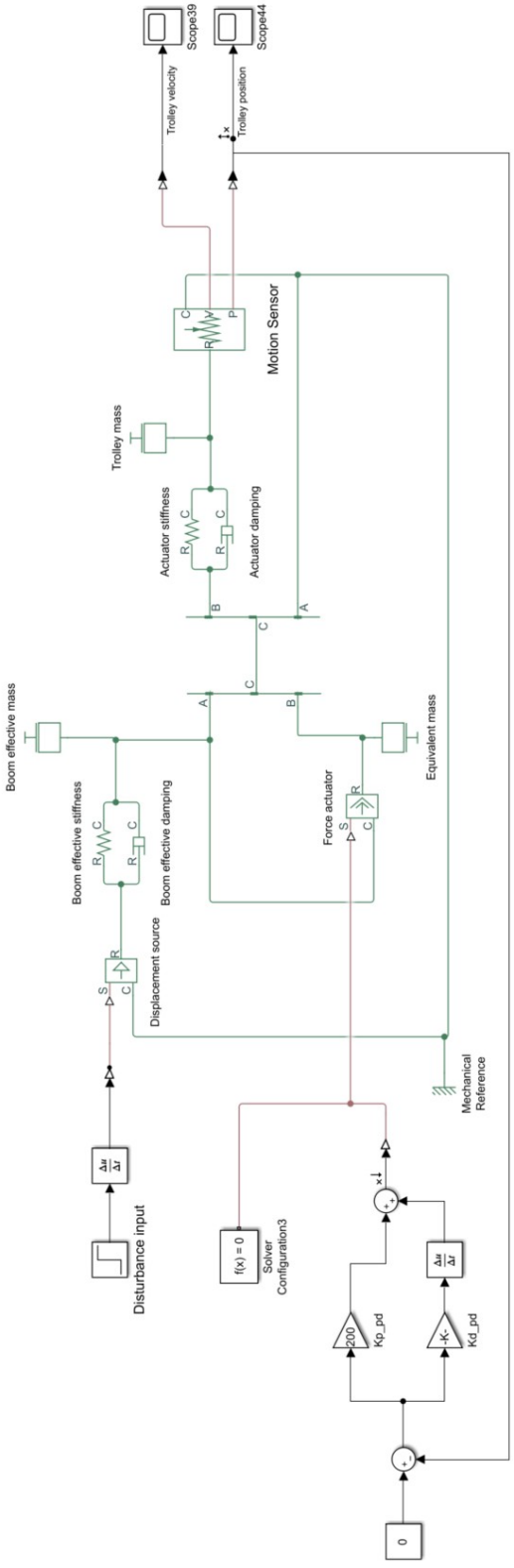

Figure D.2: Screenshot of the Simscape model with crane boom flexibilityshowing all mechanical components, controller blocks, sensors, connections and signal wirings